



SATELLITE  
OCEANOGRAPHIC  
CONSULTANTS



**National  
Oceanography Centre**  
NATURAL ENVIRONMENT RESEARCH COUNCIL



## EUROPEAN SPACE AGENCY (ESA) CONTRACT REPORT

The work described in this report was done under ESA contract.  
Responsibility for the contents resides in the author or organisation that prepared it.

# SAMOSA CCN Final Project Report

|                        |      |               |            |
|------------------------|------|---------------|------------|
| Deliverable reference: | D13  | Work Package: | WP1000     |
| Version:               | V1.3 | Date:         | 06/02/2012 |

|                     |   |                         |   |
|---------------------|---|-------------------------|---|
| Subject:            | SAMOSA CCN D13 Final Project Report   |                         |   |
| Contractor:         | SatOc Ltd,UK  | Contractor's Reference: |   |
| ESA Contract No:    | AO/1-5571/07/NL/ST  | ESA CR() No:            |   |
| No. of Volumes:     | X   | This is Volume No:      | X |
| ESA STUDY MANAGER:  | Jérôme Benveniste   |                         |   |
| DIVISION:           | STSE  |                         |   |
| DIRECTORATE:        | Directorate of the Earth Observation Programmes   |                         |   |
| ESA BUDGET HEADING: | ESA Budget Heading  |                         |   |
| ABSTRACT:           | <p>This document corresponds to SAMOSA CCN D13 Final Project Report. It includes a description of the main achievements in the SAMOSA and SAMOSA CCN contract, as well as the main conclusions reached under the SAMOSA CCN. Furthermore, it adds an executive summary of the SAMOSA project.</p> |                         |   |

|                     |                                     |              |                   |
|---------------------|-------------------------------------|--------------|-------------------|
| <b>Prepared by:</b> | _____                               | <b>Date:</b> | <b>06/02/2012</b> |
|                     | David Cotton & Cristina Martin-Puig |              |                   |
| <b>Checked by:</b>  | _____                               | <b>Date:</b> | _____             |
|                     | David Cotton                        |              |                   |
| <b>Approved by:</b> | _____                               | <b>Date:</b> | _____             |
|                     | David Cotton                        |              |                   |
| <b>Released by:</b> | _____                               | <b>Date:</b> | _____             |
|                     | David Cotton                        |              |                   |

*The copyright in this document is vested in SAMOSA project partners This document may only be reproduced in whole or in part, or stored in a retrieval system, or transmitted in any form (electronic, mechanical, photocopying or otherwise), only with the prior written permission of All SAMOSA project partners*

[ This page is intentionally left blank]

*The copyright in this document is vested in SAMOSA project partners This document may only be reproduced in whole or in part, or stored in a retrieval system, or transmitted in any form (electronic, mechanical, photocopying or otherwise), only with the prior written permission of All SAMOSA project partners*

## AUTHOR/MANAGER/COLLABORATION LIST

| Main Author(s)         | Affiliation |
|------------------------|-------------|
| Philippa Berry         | DMU         |
| David Cotton           | SatOC       |
| Christine Gommenginger | NOC         |
| Cristina Martin-Puig   | STARLAB     |
| Chris Ray              | STARLAB     |
| Lars Stenseng          | DTU         |
| Collaborator(s)        | Affiliation |
| R. K. Raney            | APL - JHU   |

## DISTRIBUTION LIST

| Distribution Record |             |      |        |
|---------------------|-------------|------|--------|
| Sent to             | Affiliation | Date | Format |
|                     |             |      |        |
|                     |             |      |        |
|                     |             |      |        |

*The copyright in this document is vested in SAMOSA project partners. This document may only be reproduced in whole or in part, or stored in a retrieval system, or transmitted in any form (electronic, mechanical, photocopying or otherwise), only with the prior written permission of All SAMOSA project partners.*

## CHANGE RECORD

| Change Record |                            |  |                                      |
|---------------|----------------------------|--|--------------------------------------|
| Issue         | Date                       | Changes made   | Author                               |
| 0.01          | 11 <sup>th</sup> May 2011  | First Final Report Draft including contributions from SAMOSA partners                                    | Cristina Martin-Puig                 |
| 0.02          | 12 <sup>th</sup> May 2011  | Review of SAMOSA partners contributions and executive summary addition                                   | Cristina Martin-Puig                 |
| 0.03          | 13 <sup>th</sup> May 2011  | SatOC and STARLAB's final review of the Final Report first draft   | David Cotton<br>Cristina Martin-Puig |
| 0.1           | 13 <sup>th</sup> May 2011  | Approval of modifications  | Cristina Martin-Puig                 |
| 0.2           | 25 <sup>th</sup> May 2011  | Addition of: SAMOSA partners logos; NOC contributions; review recommendations for improvement from SatOC | Cristina Martin-Puig                 |
| 1             | 30 <sup>th</sup> June 2011 | General Edit, First Public Issue   | David Cotton                         |
| 1.3           | 6 <sup>TH</sup> Feb 2012   | A number of minor corrections following review by partners and ESA.<br>Addition of Annexes               | David Cotton                         |

*The copyright in this document is vested in SAMOSA project partners This document may only be reproduced in whole or in part, or stored in a retrieval system, or transmitted in any form (electronic, mechanical, photocopying or otherwise), only with the prior written permission of All SAMOSA project partners*

# Executive Summary

The application of Synthetic Aperture Radar (SAR) techniques to nadir-pointing radar altimetry offers the potential to significantly enhance Earth surface mapping. CryoSat-2 is the first satellite to provide such data. Although its primary mission aim is cryospheric applications, Cryosat-2 data shall be of great interest to the hydrosphere and oceanographic communities as they will allow the first quantitative assessment of the enhanced capabilities offered by SAR altimetry for high-resolution sea surface height measurements, coastal monitoring, ocean floor topography mapping, gravity field and inland water monitoring.

SAR altimetry was first proposed and described as Delay Doppler Radar Altimetry (DDA) by [RAN1998].

The key innovation is the addition of along-track SAR processing that leads to increased resolution and improved signal-to-noise ratio through enhanced multi-looking. The technique requires echo delay compensation, analogous to range cell migration correction in conventional SAR [RAN1994]. With this innovation, finer spatial resolution is achieved in the along-track dimension. Accumulation of more statistically independent looks for each scattering area leads to better Speckle reduction, and hence higher precision in altimetric height measurements.

The SAMOSA project team is led by Satellite Oceanographic Consultants (SatOC,UK) and includes four additional scientific partners with a high level of relevant experience: The Danish University of Technology (DTU, Denmark), De Montfort University (DMU,UK), the National Oceanography Centre (NOC, UK) and Starlab Barcelona S.L (STARLAB, Spain). This consortium, with the external participation of Dr. R.K. Raney (Applied Physics Laboratory at the Johns Hopkins University, USA), has been working on the analysis of the potential capabilities of SAR Altimetry over ocean and inland water surfaces.

The project team succeeded in defining novel retracking techniques for SAR Mode (SARM) altimeter echoes over water surfaces and in evaluating the performance of SARM altimetry compared to conventional pulse-limited altimetry. The performance of SARM in terms of range retrieval accuracy was analysed by retracking simulated Cryosat data, airborne data and CryoSat-2 data, and with estimates of achievable precision of SARM through the Cramér-Rao Lower Bound (CRLB) method. In addition, the “Berry Expert System” (BEST) was applied to simulated data over complex inland water scenarios to assess SARM performance over lakes, estuarine and wetlands.

The SAMOSA project led to the definition of two new theoretical models for SAR waveforms over water. The first model (“SAMOSA1”) assumes Gaussian ocean wave statistics and a circular antenna pattern, and includes the effect of Earth curvature and antenna mispointing in the along track direction only. An enhancement of the SAMOSA1 formulation (“SAMOSA1\_Enhanced”) addresses numerical singularities in the trailing edge of the SAMOSA1 SAR waveforms in low sea state conditions. The SAMOSA1 Enhancement allows waveform fitting to use data over the full gate range and produces an almost ten-fold reduction in computation time. The SAMOSA2 SAR model is a more complex formulation that includes non-Gaussian ocean wave statistics, Earth curvature and a better representation of mispointing effects both along- and across-track. The SAMOSA2 model also comprises radial velocity effects and an elliptical antenna pattern. All SAMOSA theoretical models were implemented as SAR ocean retrackers and applied successfully to simulated and CryoSat-2 SAR waveforms.

The SAMOSA1 SAR ocean retracker was documented in a Detailed Processing Model (DPM; GOM2011) in support of the Sentinel-3 Surface Topography Mission (S-3 STM). The DPM was based on the original SAMOSA1 formulation and did not include the more recent enhancements of the SAMOSA1 model in low sea states.

Waveform retracking applied to simulated Cryosat data over ocean surfaces allowed for quantitative comparison of “Low Rate Mode” (LRM - conventional altimeter approach) and “SAR mode” (SARM) over identical sea state conditions. The SAMOSA1 SAR ocean retracker was applied to simulated SARM data to estimate the retrieval accuracy for range and significant wave height (SWH) in SAR mode, while LRM waveforms for the same ocean surfaces were retracked using a Brown-type ocean retracker. A technique was developed for the reduction of SARM data to emulate LRM and implemented in the “RDSAR” software. Retracking the “pseudo-LRM” RDSAR waveforms with a Brown-type ocean retracker showed that the RDSAR data offer the same retrieval accuracy than LRM. This work also showed an almost two-fold improvement in range retrieval with SARM compared to LRM and RDSAR, thus confirming earlier results

*The copyright in this document is vested in SAMOSA project partners This document may only be reproduced in whole or in part, or stored in a retrieval system, or transmitted in any form (electronic, mechanical, photocopying or otherwise), only with the prior written permission of All SAMOSA project partners*

from [RAN1998]. However, results with simulated data were not fully conclusive as no improvement was found in the retrieval of SWH from SARM data compared to conventional altimetry.

The SAMOSA1 ocean retracker performance was evaluated against airborne SAR altimeter data acquired with ASIRAS during the Cryovex'2006 campaign. Over 96% of the waveforms were successfully fitted by the SAMOSA1 model when the ASIRAS data was processed to have 64 pulses per burst and a maximum look angle of 1.4 degrees.

The SAMOSA1 Enhanced model was used to successfully retrack real Cryosat-2 SAR waveform data from different oceanic regions. The retrieval accuracy of SAR and LRM in different sea states was estimated for range and significant wave height using Cryosat-2 SAR and Jason-2 LRM data from a small region of the Norwegian Sea between July 2010 and March 2011. Results confirmed a marked, almost two-fold, improvement in range retrieval accuracy with Cryosat-2 SAR compared to Jason-2 LRM. Results also indicated that retrieval of significant wave height is at least as good for SARM as for LRM, although SARM overestimated SWH slightly compared to LRM, particularly in low sea states.

The SAMOSA2 waveform model was also implemented as a SAR ocean retracker and applied to simulated data and a small number of CryoSat-2 L1B SAR waveforms. The SAMOSA2 waveform model being more complex, it required longer computation time than SAMOSA1. Consequently, there was insufficient time within the project schedule to fully evaluate the performance of the SAMOSA2 retracker against Cryosat-2 data. Results with SAMOSA2 applied to simulated SAR data confirmed the findings with SAMOSA1 of an approximately two-fold improvement in range retrieval accuracy with SAR compared to LRM. Analytical solutions have been identified to speed-up the computation of SAMOSA2 and could be incorporated in future implementations.

The performance of both SAMOSA1 and SAMOSA2 models were evaluated numerically in terms of precision with Cramér-Rao Lower Bound techniques. The SAMOSA2 model was found to be more robust than SAMOSA1. The impact of the various model improvements was investigated and quantified separately in terms of their effect on the precision of range retrieval. The modification of the model to include non-Gaussian ocean statistics had the greatest effect on precision. However, the change in precision resulting from these improvements was found to be small in terms of the overall precision error budget.

Simulated LRM and SARM data were obtained also for scenarios representing inland waters, including a lake scenario, an estuarine scenario and a wetland scenario. These were processed with BEST and successful retracking of the SAR waveforms (more than 62% for the wetland, and up to 85% for the lake scenario) and recovery of small-scale topographic features was demonstrated, although the waveforms did not conform to the expected shapes (specifically in the case of  $\sigma_0$  response) in the case of the wetland simulations. Real Cryosat-2 data over the Mekong Delta region were recovered and processed, and the waveform shapes for these data were found to conform to expectation. Over 58% of the waveforms could be re-tracked without averaging though significant mirroring was found in the waveforms which impacted the re-tracking

In summary, the SAMOSA project successfully demonstrated the potential improvements offered by SAR mode altimetry over water surfaces. Through the development of new theoretical models for SAR waveforms over water and their application as SAR ocean altimeter retracker to simulated and real Cryosat-2 L1B SAR data, SAMOSA confirmed earlier expectations of improvement in range retrieval accuracy and finer along-track spatial resolution.

A number of issues have emerged where further work is recommended, including: a more efficient software implementation of the SAMOSA2 retracker; validation and testing of the SAMOSA SAR retracker with a wider range of Cryosat-2 data co-located with ground truth or other reference data; updating the DPM to include (at least) the SAMOSA1 Enhancement to resolve the numerical singularities at low wave heights and allow retracking over the full range of waveform gates. It is also recommended that the SAMOSA results with simulated Cryosat data should be cross-validated against output from the Sentinel-3 mission simulator for the same scenarios, and that the SAMOSA SAR ocean retracking method are tested against other retrieval approaches in a benchmark exercise. Finally, the RDSAR technique to reduce SAR mode to Low Rate mode data should be validated using real data, to prepare for its application to Sentinel-3 data and provide continuity over the altimeter SAR/LRM mode transitions.

*The copyright in this document is vested in SAMOSA project partners This document may only be reproduced in whole or in part, or stored in a retrieval system, or transmitted in any form (electronic, mechanical, photocopying or otherwise), only with the prior written permission of All SAMOSA project partners*

# Table of Contents

|   |           |
|---|-----------|
| <b>ILLUSTRATION INDEX</b> .....   | <b>8</b>  |
| <b>1 PROJECT OVERVIEW</b> .....   | <b>10</b> |
| <b>2 NEW APPROACH FOR RETRACKING SAR MODE DATA OVER WATER</b> .....   | <b>11</b> |
| 2.1 ON CREATING “CONVENTIONAL” ALTIMETER DATA FROM SARM OPERATION: WHY AND HOW (STARLAB) .....  | 11        |
| <b>3 DEVELOPMENT OF THE SARM WAVEFORM MODEL FOR RE-TRACKING</b> .....   | <b>13</b> |
| 3.1 ON DERIVING A NEW SARM WAVEFORM MODEL (STARLAB) .....   | 13        |
| 3.2 THEORETICAL ASSESSMENT OF SAMOSA WAVEFORM MODEL PRECISION PERFORMANCE (STARLAB) .....   | 15        |
| <b>4 SAMOSA SAR OCEAN RETRACKERS PERFORMANCE</b> .....  | <b>18</b> |
| 4.1 RANGE RETRIEVAL ACCURACY IN LRM, RDSAR AND SAR MODE WITH THE SAMOSA1 SAR OCEAN RETRACKER FROM SIMULATED CRYOSAT DATA (NOC) .....  | 18        |
| 4.2 IMPROVEMENT OF SAMOSA1 RETRACKER IN LOW WAVE HEIGHT CONDITIONS (NOC) .....  | 20        |
| 4.3 APPLICATION OF THE SAMOSA1 RETRACKER TO CRYOSAT-2 SARM DATA (NOC) .....   | 22        |
| 4.4 SAMOSA1 RETRACKER PERFORMANCE WITH ASIRAS DATA (DTU) .....  | 27        |
| 4.5 IMPLEMENTATION OF THE SAMOSA2 MODEL AS A SAR OCEAN RETRACKER AND MISPOINTING EFFECTS (NOC) .....  | 30        |
| 4.6 RANGE RETRIEVAL ACCURACY IN LRM AND SAR MODE FROM COMPUTER SIMULATIONS WITH THE SAMOSA2 RETRACKER (NOC) .....   | 31        |
| 4.7 APPLICATION OF THE SAMOSA2 RETRACKER TO CRYOSAT-2 SAR DATA (NOC) .....  | 35        |
| <b>5 SARM ALTIMETRY OVER IN LAND WATERS (DMU)</b> .....   | <b>36</b> |
| <b>6 CONCLUSIONS</b> .....  | <b>42</b> |
| 6.1 SUMMARY OF RESULTS .....  | 42        |
| 6.2 RECOMMENDATIONS FOR FURTHER WORK .....  | 43        |
| 6.3 ACKNOWLEDGEMENTS .....  | 44        |
| <b>BIBLIOGRAPHY</b> .....   | <b>45</b> |
| <b>LIST OF SAMOSA PUBLICATIONS</b> .....  | <b>46</b> |
| <b>ANNEX 1: COMMENTARY ON THE SAMOSA PROJECT, FINAL PRESENTATION BY DR R. K. RANEY</b> .....  | <b>47</b> |
| <b>ANNEX 2: AN ANNOTATED BIBLIOGRAPHY: SELECTED MILESTONES OF OCEANIC RADAR ALTIMETRY LEADING TO FINER HEIGHT PRECISION AND THE CRYOSAT HERITAGE BY DR R. K. RANEY,</b> ..... | <b>49</b> |

*The copyright in this document is vested in SAMOSA project partners This document may only be reproduced in whole or in part, or stored in a retrieval system, or transmitted in any form (electronic, mechanical, photocopying or otherwise), only with the prior written permission of All SAMOSA project partners*

## Illustration Index

|   |                                     |
|---|-------------------------------------|
| Figure 1 SAMOSA2 waveform model basis functions .....   | 14                                  |
| Figure 2: Range precision as a function of SWH derived using CRLB for SAMOSA1 and SAMOSA2 retrackers. ....  | 16                                  |
| Figure 3 Precision difference between SAMOSA2 with individual modifications and SAMOSA2 plain.. ....  | 17                                  |
| Figure 4 Precision for SAMOSA2 with non-Gaussian sea surface for different skewness values .....  | 17                                  |
| Figure 5 Simulated DEM SWH and retracked SWH for LRM, pseudo-LRM and SARM) for the three scenarios over ocean. ....   | 19                                  |
| Figure 6: Range retrieval accuracy as a function of SWH in LRM, pseudo-LRM and SARM based on simulated data over ocean. ....  | 20                                  |
| Figure 7: SAMOSA1 Multi-looked waveforms for various SWH conditions for the original formulation and the extended analytical solution. ....   | 21                                  |
| Figure 8: SAMOSA1 SAR retracker results for simulated scenario SMC1 using the original SAMOSA1 model formulation and the improved analytical solution.. ....  | 22                                  |
| Figure 9: L1B SARM data track over the Agulhas region.....  | 23                                  |
| Figure 10: Retracked SAR results, showing L1B SAR waveforms; relative range; retrieved SAR SWH; satellite to surface range; Satellite_height minus range in metres .....  | 24                                  |
| Figure 11: Retrieved SAMOSA1 SWH and absolute range anomaly for Cryosat2 L1B SAR data over a small region of the Norwegian Sea between July 2010 and March 2011.....  | 25                                  |
| Figure 12: Retrieved SAMOSA1 SWH absolute range anomaly for Jason2 LRM data over small region of the Norwegian sea between July 2010 and March 2011. ....   | 25                                  |
| Figure 13: Retrieval accuracy at 20Hz for SWH and absolute range anomaly as a function of Significant Wave Height for Jason-2 LRM and Cryosat-2 SAR for data in a small region of the Norwegian Sea between July 2010 and March 2011. The Cryosat-2 SAR data were retracked with the SAMOSA1 Extended model. .... | 26                                  |
| Figure 14: Example of ASIRAS waveform and fitted SAMOSA1 waveform .....   | 28                                  |
| Figure 15: Estimated surface elevation and 100 samples running average.....   | 29                                  |
| Figure 16: Estimated SWH along the profile and 100 samples running average. ....  | 29                                  |
| Figure 17: SAMOSA2 Single-look Delay Doppler maps for SWH = 3m, latitude = 45° and various values of along track mispointing.....   | 30                                  |
| Figure 18: SAMOSA2 Single-look Delay Doppler maps for SWH = 1m, latitude = 45° and various values of along track mispointing.....   | 31                                  |
| Figure 19: Multi-looked SAR waveforms in the absence of mispointing for SWH equal to 1m, 2m, and 3m for simulated Cryosat L1B SAR data from S3U7 scenario, SAMOSA1 model and the SAMOSA2 model. ....  | 33                                  |
| Figure 20: Relative range retrieved from simulated Cryosat products for scenarios S3U7 and S3U9.....  | 34                                  |
| Figure 21: Range retrieval accuracy (in m) as a function of SWH for LRM and SAMOSA2 model with mispointing retrieval). The results are based on simulated Cryosat data for scenarios S3U7 (no mispointing) and S3U9 (mispointing = 0.05°).....  | 35                                  |
| Figure 22: DEM for Lakes Scenario .....   | 36                                  |
| Figure 23: Sigma0 for lakes scenario .....  | 36                                  |
| Figure 24: Retrieved heights from 20Hz SAR waveforms with DEM input heights .....   | 37                                  |
| Figure 25: Model inputs for estuarine scenario: DEM and sigma0).....  | 38                                  |
| Figure 26: Height retrieval from computer simulated 20Hz data: estuarine scenario compared with input DEM .....   | 38                                  |
| Figure 27: SAR Full Bit Rate (no waveform averaging) retracked heights with DEM heights. ....   | 39                                  |
| Figure 28: Cryosat-2 LRM waveform sequence .....  | <b>Error! Bookmark not defined.</b> |

*The copyright in this document is vested in SAMOSA project partners This document may only be reproduced in whole or in part, or stored in a retrieval system, or transmitted in any form (electronic, mechanical, photocopying or otherwise), only with the prior written permission of All SAMOSA project partners*

# Acronyms and Abbreviations

|            |  |
|------------|--|
| AGC        | Automatic Gain Control   |
| ASIRAS     | Airborne SAR Interferometric Altimeter System  |
| BEST       | Berry Expert SysTem  |
| CCN        | Contract Change Notice   |
| CRLB       | Cramér-Rao Lower Bound   |
| CRYMPS     | CRYoSat Mission Performance Simulator  |
| DDA        | Delay-Doppler Altimeter  |
| DEM        | Digital Elevation Model – The surface description used as input for the computer simulations |
| ECMWF      | European Centre for Medium-range Weather Forecasts   |
| FBR        | Full Bit Rate  |
| FFT        | Fast Fourier Transform   |
| IFFT       | Inverse Fast Fourier Transform   |
| LRM        | Low Resolution Mode  |
| MLE        | Maximum Likelihood Estimator   |
| PRF        | Pulse Repetition Frequency   |
| RDSAR      | ReDuced SAR  |
| SAR        | Synthetic Aperture Radar   |
| SARM       | SAR Mode   |
| SIRAL      | SAR Interferometric Radar Altimeter - the altimeter deployed on Cryosat-2                    |
| SNR        | Signal to Noise Ratio  |
| SWH        | Significant Wave Height  |
| $\sigma^0$ | Surface Backscatter coefficient at normal incidence  |

*The copyright in this document is vested in SAMOSA project partners. This document may only be reproduced in whole or in part, or stored in a retrieval system, or transmitted in any form (electronic, mechanical, photocopying or otherwise), only with the prior written permission of All SAMOSA project partners.*

# 1 Project Overview

The application of Synthetic Aperture Radar (SAR) techniques to nadir-pointing radar altimetry offers the potential to significantly enhance Earth surface mapping. CryoSat-2 is the first satellite to provide such data. Although its primary mission aim is cryospheric applications, Cryosat-2 data shall be of great interest to the hydrosphere and oceanographic communities as they will allow the first quantitative assessment of the enhanced capabilities offered by SAR altimetry for high-resolution sea surface height measurements, coastal monitoring, ocean floor topography mapping, gravity field and inland water monitoring.

SAR altimetry was first proposed and described as Delay Doppler Radar Altimetry (DDA) by [RAN1998].

The key innovation is the addition of along-track SAR processing that leads to increased resolution and improved signal-to-noise ratio through enhanced multi-looking. The technique requires echo delay compensation, analogous to range cell migration correction in conventional SAR [RAN1994]. With this innovation, finer spatial resolution is achieved in the along-track dimension. Accumulation of more statistically independent looks for each scattering area leads to better Speckle reduction, and hence higher precision in altimetric height measurements.

The SAMOSA project team is led by Satellite Oceanographic Consultants (SatOC,UK) and includes four additional scientific partners with a high level of relevant experience: The Danish University of Technology (DTU, Denmark), De Montfort University (DMU,UK), the National Oceanography Centre (NOC, UK) and Starlab Barcelona S.L (STARLAB, Spain). This consortium, with the external participation of Dr. R.K. Raney (Applied Physics Laboratory at the Johns Hopkins University, USA), has been working on the analysis of the potential capabilities of SAR Altimetry over ocean and inland water surfaces.

The major activities undertaken in SAMOSA include:

- The development of new theoretical models to retrack SAR Mode (SARM) waveforms.
- The application of SAR ocean retracers to simulated Cryosat SAR waveforms, ASIRAS airborne data and Cryosat-2 L1B SAR waveforms.
- The development of a Detailed Processing Model for a SAR ocean retracker in support of preparations for the Sentinel-3 Surface Topography Mission.
- Analyses of simulated Cryosat data in SARM and LRM over open-ocean and inland water, including data over the coastal zone, estuaries, rivers and lakes.
- The development of the RDSAR averaging methodology to reduce SARM to pseudo-LRM data.
- The analyses of the retrieval accuracy for range and significant wave height in different sea states with SARM and LRM, using simulated Cryosat data and measurements from Cryosat-2 SARM and Jason-2 LRM.
- Analyses of SARM over complex inland water surfaces and its finer along-track spatial resolution.

The original SAMOSA contract was extended under a Contract Change Notice (CCN) to build on the theoretical understanding and practical experience gained within the initial work to develop algorithms and tools needed for the CryoSat-2 and Sentinel-3 missions.

The following sections provide a summary of the main conclusions reached under the SAMOSA original contract and a detailed description of the main achievements in SAMOSA CCN.

*The copyright in this document is vested in SAMOSA project partners This document may only be reproduced in whole or in part, or stored in a retrieval system, or transmitted in any form (electronic, mechanical, photocopying or otherwise), only with the prior written permission of All SAMOSA project partners*

## 2 New approach for retracking SAR mode data over water

### 2.1 On creating “Conventional” Altimeter data from SARM operation: why and how (STARLAB)

SIRAL, the new altimeter designed for CryoSat-2, has three operational modes: the Low Resolution Mode (LRM), or conventional altimeter mode, the Synthetic Aperture Radar mode (SARM) and the interferometric mode (SARin). The first two modes are of interest for the work undertaken by the SAMOSA team. The altimeter modes on CryoSat-2 are mutually exclusive, and so it is not possible to make a direct quantitative comparison of the modes over the same region at the same instant. Therefore, a successful reduction of SAR mode Full Bit Rate (FBR) data to emulate “conventional” LRM data would allow for such comparison over identical sea state conditions. Moreover, this approach would allow the application of LRM technology for on board tracking of SARM data.

SARM and LRM transmit identical pulses. The main difference between these two modes is their Pulse Repetition Frequency (PRF) and its associated effects: pulse-to-pulse correlation and decorrelation.

One potential solution, which has shown promising results, is to intelligently select SARM echoes such that the sequence achieved has a pulse-to-pulse PRF equivalent to LRM. Therefore, the aim is to select one every  $m$  SARM echoes such that the resulting sequence has a PRF equivalent to LRM. This shall be sufficient to ensure pulse-to-pulse decorrelation. For such solution, the calculation of  $m$  is achieved by:

$$m = \frac{PRF_{SARM}}{PRF_{LRM}} \quad (1)$$

If this is calculated for CryoSat-2 the resulting value of  $m$  is close to 9. Therefore, each burst<sup>1</sup> results in 8 decorrelated waveforms.

For an identical time window choosing one in every nine complex SARM waveforms results in a sequence with a smaller number of independent waveforms than its equivalent LRM sequence. We defined the reduced sequence as “pseudo”-LRM<sup>2</sup>. It is so-called because there are gaps between the reception of echoes from the bursts in SARM. While in LRM the altimeter is constantly transmitting and receiving pulses at a PRF of 1970Hz, this is not the case for SARM, in which a set of 64 pulses is transmitted and the altimeter then switches to reception mode until the next burst is transmitted. Therefore, it was necessary to define a methodology which compensates for the unequal number of pulses between modes. Investigations led to the development of three different methodologies in the original SAMOSA contract, described below, and to the definition of the final methodology, which is currently implemented in the RDSAR software developed by STARLAB [CMP2010].

The SARM FBR data comprises individual complex (I and Q) components, and thus these data need to be further processed before they can be tracked. The missing steps to convert the data into a form suitable for tracking are:

1. apply window delay correction
2. apply AGC compensation
3. transform data to frequency domain (IFFT)
4. transform data to power
5. incoherently integrate waveforms at a rate approximately 20Hz

The first two were not developed for the initial RDSAR approach, but were included in the later work (under the SAMOSA CCN). The main reason for not including them in the SAMOSA original contract was based on the fact that we did not get confirmation of these steps to be applied to the simulated datasets in due time. All of the above steps are implemented in the current versions of the RDSAR software. Additional

---

<sup>1</sup> Set of 64 pulses transmitted at a high PRF ( 17.8 KHz for CryoSat-2)

<sup>2</sup> We acknowledge R.K. Raney for the first use of this word to refer to the reduced SARM FBR sequence.

*The copyright in this document is vested in SAMOSA project partners This document may only be reproduced in whole or in part, or stored in a retrieval system, or transmitted in any form (electronic, mechanical, photocopying or otherwise), only with the prior written permission of All SAMOSA project partners*

steps to the list were tried in order to preserve an equal number of pulses. The different methodologies that were tried are described below:

The first methodology consisted of a coherent pre-summing of “ $n$ ” SARM FBR echoes every  $m$  echoes within a burst ( $n = m - 1$ ) followed by a transformation of the data into the frequency domain. The resulting sequence, after coherent pre-summing, was inverse Fourier transformed, converted to power and an incoherent integration was applied at an approximately 20Hz rate. Unfortunately, this method led to very peaky waveforms, which could not be retracked with a conventional altimeter retracker.

The second methodology was based on taking the Fourier transform in the azimuth direction across the data at a constant range over each burst. This would redistribute samples per Doppler bin. Provided that the resulting waveforms do not reside in adjacent Doppler bins, they would statistically be independent. The result of such transformation was again a very peaky waveform resulting from an asymmetric footprint, rather than from a pulse-to-pulse correlation (as above).

The third approach relied on the same principles as the first, but did not include pre-summing. Therefore, one in every nine SAR FBR echoes were chosen to generate the pseudo-LRM sequence. This approach produced promising results, but the number of incoherent echoes from the pseudo-LRM was fewer than that in the equivalent LRM sequence.

The approach finally applied was a development of the third method described above to allow for unequal number of pulses in the pseudo-LRM, and “true” LRM sequences. Analysis of computer simulations of scenarios with constant sea state showed that in order to achieve equal number of pulses for a one second interval of LRM data it was necessary to reduce 3 seconds of SARM FBR data to pseudo-LRM. This methodology also allows for incoherent pre-summing of the “ $n$ ” waveforms in between independent echoes. The RDSAR software allows the user to choose whether to perform incoherent summation, and to select the value of “ $n$ ”.

Before applying the RDSAR software to CryoSat-2 data it was necessary to demonstrate that statistical equivalence was preserved between the LRM and pseudo-LRM sequences for a constant sea state scenario. The analysis confirmed statistical equivalence of the sequences.

Simulation results showing the performance of RDSAR are provided in Section 4.1.

### 3 Development of the SARM waveform model for re-tracking

#### 3.1 On deriving a new SARM waveform model (STARLAB)

The shape of SARM return echoes is significantly different from the “Brown-style” waveform of a conventional altimetry, and so a re-tracker designed for a Brown-style waveform cannot be expected to work on SARM datasets unless a transformation is applied. Thus before a re-tracking approach could be developed, a theoretical model for the SARM waveform was needed. The approach used, and described below, was similar to that of [BRO1977] and [HAY1980].

The initial approach, the SAMOSA1 waveform model, applied some simplifications and assumptions: Gaussian ocean statistics, circular antenna pattern, allowing only for curvature effects along track and not accounting for radial velocity effects. As for conventional altimetry, it was demonstrated that the SARM waveform can be expressed as the convolution of three terms [CMP2008]:

$$W(\tau, \text{Doppler}_{bin}) = P_{FS}(\tau, \text{Doppler}_{bin}) * S_R(\tau, \text{Doppler}_{bin}) * \left(\frac{c}{2}\right) P_z\left(\frac{c\tau}{2}\right) \quad (2)$$

Where:

- $\tau$  corresponds to the range gate
- $\text{Doppler}_{bin}$  to the Doppler frequency
- $P_{FS}$  to the flat surface impulse response
- $S_R$  to the system point target response
- and  $P_z$  the surface elevation probability density function

Expressions for each of the previous parameters, as well as the analytical expression, are provided in [CMP2009].

This model has shown promising results, as presented in section 4.1 below, but the SAMOSA team jointly with the Agency decided to improve it in order to account for:

- non-Gaussian ocean statistics
- elliptical antenna pattern
- curvature effects across-track
- radial velocity effects
- effects of mispointing across-track to the waveform shape

The new waveform model, hereafter referred as SAMOSA2 waveform model is described in detail in [RAY2011].

The effect of non-Gaussian sea statistics leads to a substantial increase in the complexity of the analytical form of the waveform. The added terms of the approximation are all proportional to the skewness factor. The final waveform was expressed as a first order power expansion in the skewness factor of the sea state. It was found that the waveform could be expressed as a sum of a family of five base functions (see Eq 3.).

$$f_n(\xi) = \int_0^{\infty} (\xi - u^2)^n e^{-(\xi - u^2)^2 / 2} du \quad (3)$$

*The copyright in this document is vested in SAMOSA project partners This document may only be reproduced in whole or in part, or stored in a retrieval system, or transmitted in any form (electronic, mechanical, photocopying or otherwise), only with the prior written permission of All SAMOSA project partners*

It is important to note that the base functions do not depend on any of the parameters of the system, and are thus completely independent.

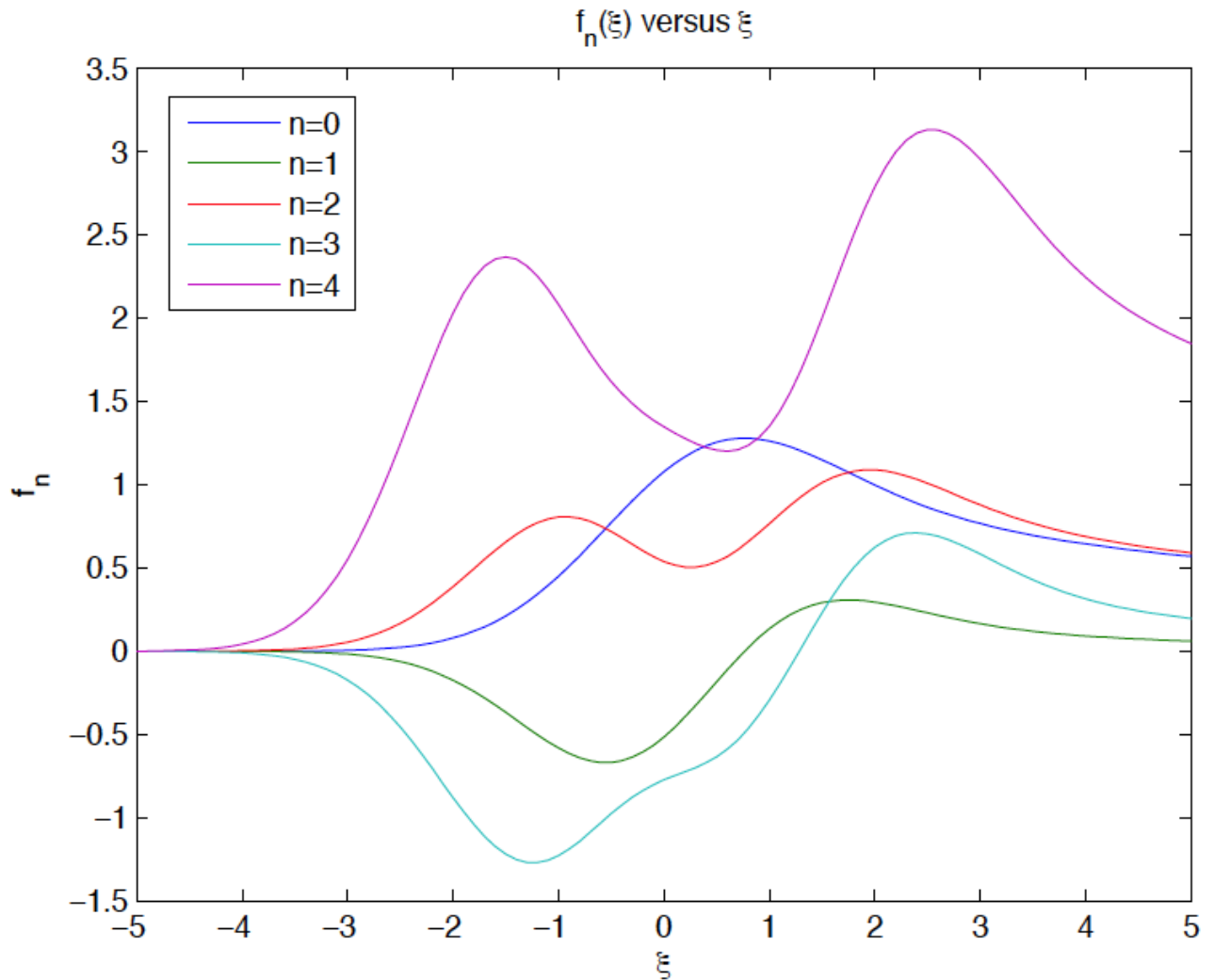


**Figure 1 SAMOSA2 waveform model basis functions**

There are two zeroth order terms (skewness invariant),  $f_0$  and  $f_1$ . The  $f_0$  term is the major contributor to the waveform in all cases. The second term, which is related to the variation of the antenna gain over a resolved cell on the sea surface is of the order to 100 times smaller than the principal term when the significant wave height is 2 metres. The other terms in the expansion are all proportional to the skewness factor. In addition, there are also other multiplicative factors that are less than 0.5, so we find that the skewness terms contribute at most 5 percent to the waveform. So it is expected that the most significant term  $f_0$  gives the waveform within a few percent in all cases, and in many cases an even larger proportion.

The consequence of including the across-track curvature of the Earth is a minor change in the constants but not in the form of the expressions.

The model now includes the effect of the satellite velocity not being parallel to the surface of the sea, given by the sea slope relative to the satellite velocity vector. This parameter has a substantial effect on the resultant waveform, causing an along track shift in the specular point, and a resultant misalignment of the antenna gain and specular point.

The analysis has been done in such a way that the shape of the beam does not need to be circular. In particular it is found that the across-track and along-track variations affect the beam in a very different way, with only the across-track variation being important. This is due to the fact that the determination of along-track position is essentially insensitive to variations in sea height.

*The copyright in this document is vested in SAMOSA project partners This document may only be reproduced in whole or in part, or stored in a retrieval system, or transmitted in any form (electronic, mechanical, photocopying or otherwise), only with the prior written permission of All SAMOSA project partners*

It has been found that the use of a windowing function (Hamming) before the FFT in the signal processing chain significantly improves the agreement between the actual and model waveforms. For this reason the waveform can be more accurately modelled if a windowing function is employed.

In addition to the improvements detailed above, we have derived the analytical expression accounting for a windowing function before the FFT in the signal processing chain, this significantly improves the agreement between the actual and model waveforms.

### **3.2 Theoretical assessment of SAMOSA waveform model precision performance (STARLAB)**

The SAMOSA team also undertook a theoretical analysis of altimetric range precision performance for different Significant Wave Height conditions for a maximum likelihood estimator (MLE) based on the analytical expressions for the waveforms provided by SAMOSA waveform models 1 and 2.

The theoretical results were achieved by applying the Cramér-Rao Lower Bound (CRLB) method to both waveform models, and showed better range precision performance from the SAMOSA2 model compared to the SAMOSA1 model.

An error budget analysis of the different waveform model improvements was undertaken to account for the:

- use of non-Gaussian sea surface statistics
- introduction of elliptical antenna pattern
- consideration of Earth curvature effects across track
- study of radial velocity effects

The SAMOSA2 waveform model has been developed at STARLAB so that the user can “switch” the model and investigate the impact of each of the improvements individually. The user can select from the above list, which improvements are of interest for each simulation. Alternatively, the user can choose to neglect all the improvements available. When all improvements are neglected, we will refer to this specific case as “model 2 plain”.

CRLB has been computed for SAMOSA1, and SAMOSA2 switched to exclude the various “improvements” (i.e. model 2 plain). Whereas it was expected that these two models would perform similarly in terms of the precision, the results show model 2 plain provides significantly better precision than model 1 (See Figure 2). Thus an analysis was made of error budgets for Model 2, comparing the effects of adding the various enhancements against the unmodified “plain” version.

These comparisons in fact showed that inclusion of some of the model “improvements” resulted in a slight but almost negligible degradation of precision performance. The inclusion of the effect of a non-Gaussian sea surface geometry had the greatest impact on precision performance (see **Figure 3**). Even so, the SAMOSA2 model accounting for Gaussian Ocean surface statistics showed an improvement of more than 2 mm in precision performance (standard deviation) with respect to the SAMOSA1 model for large values of SWH (see **Figure 2**).

Simulations for different skewness values (see **Figure 4**) show that the greater the skewness value the less precise the model becomes, although the degradation in precision is again very small.

Table 1 shows the expected precision values for the SAMOSA2 model with a signal to noise ratio of 28.48 (dB), these are the values plotted in **Figure 3**

*The copyright in this document is vested in SAMOSA project partners This document may only be reproduced in whole or in part, or stored in a retrieval system, or transmitted in any form (electronic, mechanical, photocopying or otherwise), only with the prior written permission of All SAMOSA project partners*

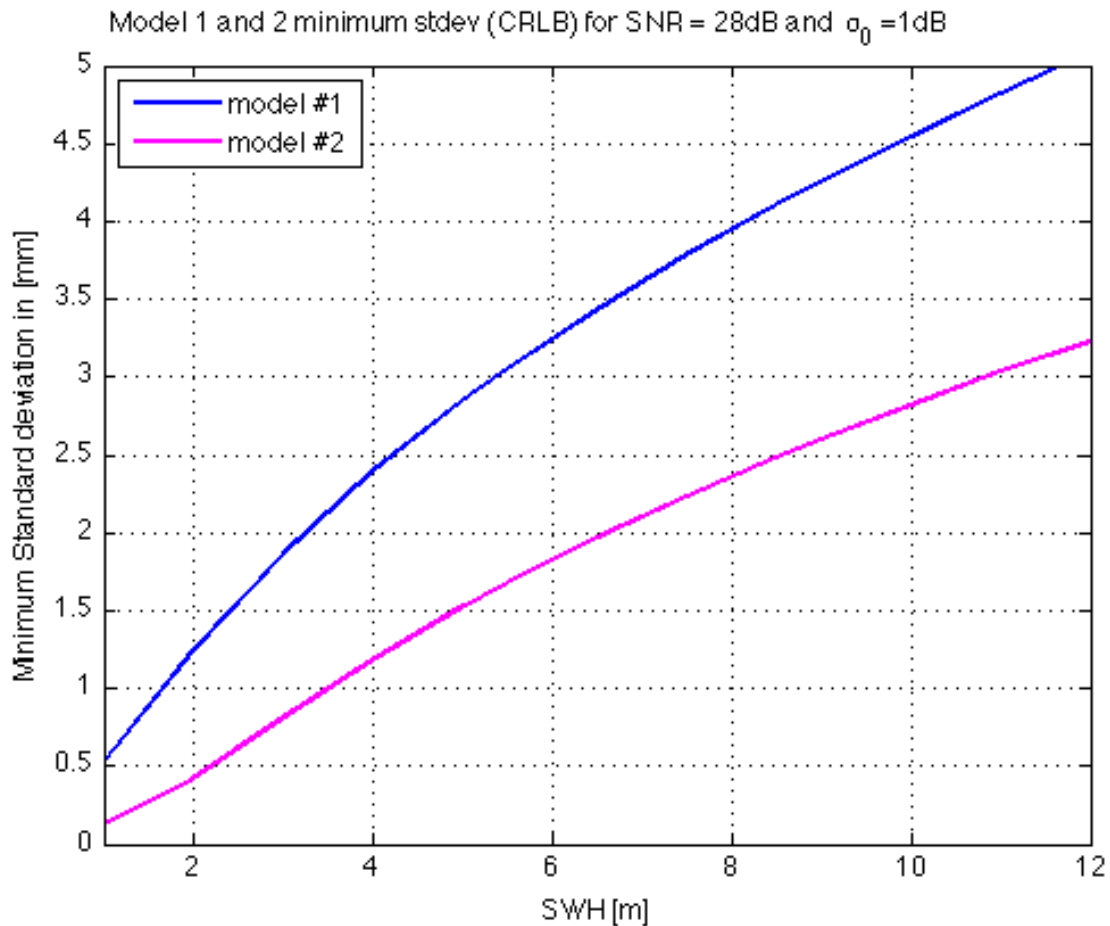


Figure 2: Range precision (standard deviation) as a function of SWH derived using CRLB for SAMOSA1 and SAMOSA2 retrackerers.

| SWH | M2 Plain | M2 Ellip | M2 Curv | Radial | Non_Gauss | All    |
|-----|----------|----------|---------|--------|-----------|--------|
| 1   | 0.0733   | 0.0734   | 0.0734  | 0.0733 | 0.0788    | 0.0789 |
| 2   | 0.2582   | 0.2583   | 0.2583  | 0.2582 | 0.2696    | 0.2698 |
| 3   | 0.4342   | 0.4345   | 0.4344  | 0.4342 | 0.4528    | 0.4533 |
| 4   | 0.5945   | 0.5951   | 0.5948  | 0.5945 | 0.6163    | 0.6174 |
| 5   | 0.7375   | 0.7384   | 0.7380  | 0.7375 | 0.7614    | 0.7628 |

Table 1 Samosa Model 2 (M2) expected precision in range retrieval (cm) for single-look waveform fitting for SNR = 28.48 dB, given for the basic model with no additional corrections, and then for each correction separately, then together.

We can conclude that SAMOSA2 is more precise than SAMOSA1. However, when the various improvements to the waveform model are included, a small and almost negligible reduction in the estimated precision in range retrieval is found for SAMOSA2 when non-Gaussian surface statistics are included in the model. This apparent degradation in performance can be explained as follows. The improved model provides a more realistic and complete representation of the physical situation. The simpler model, with less complexity, gives an unrealistically high estimate of precision. The more complete model includes additional complexity which results in an understanding that in fact the precision of range retrieval must be slightly lower than for the simpler model.

*The copyright in this document is vested in SAMOSA project partners This document may only be reproduced in whole or in part, or stored in a retrieval system, or transmitted in any form (electronic, mechanical, photocopying or otherwise), only with the prior written permission of All SAMOSA project partners*

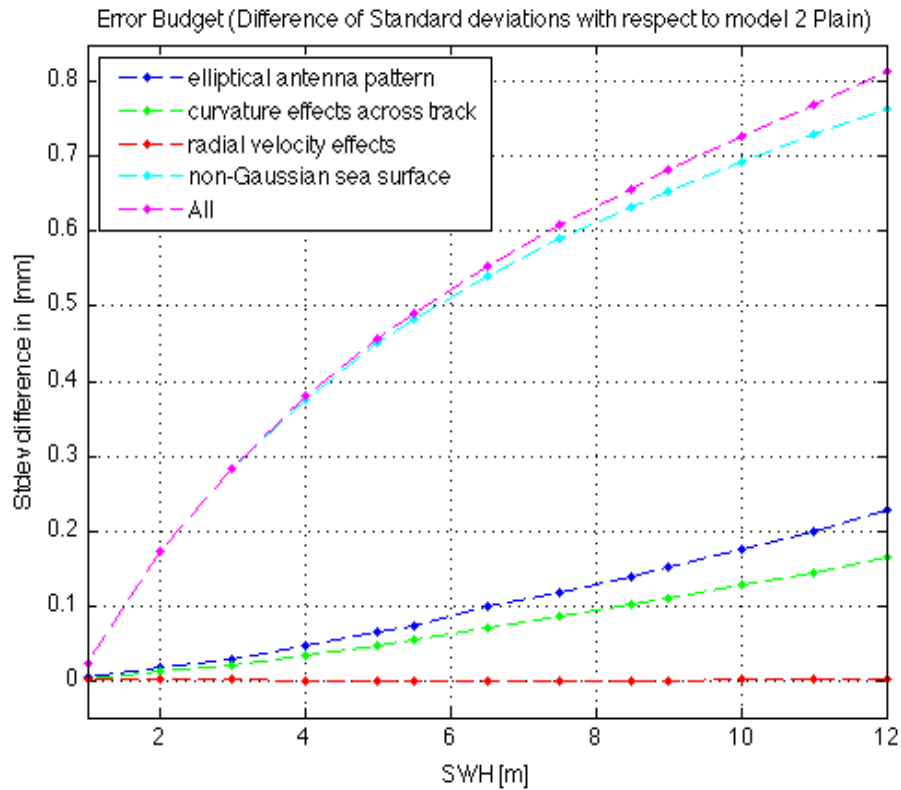


**Figure 3 Precision difference between SAMOSA2 with individual modifications and SAMOSA2 plain. For non-Gaussian Ocean statistics the skewness value is set to 0.05.**

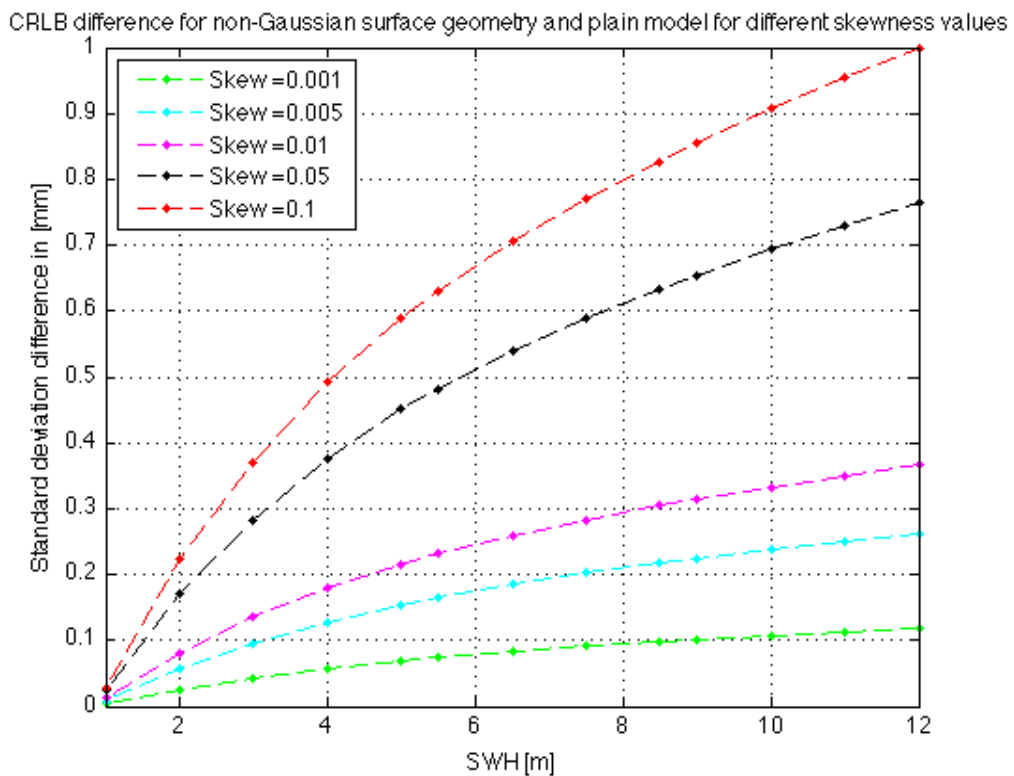


**Figure 4 Precision for SAMOSA2 with non-Gaussian sea surface for different skewness values**

*The copyright in this document is vested in SAMOSA project partners This document may only be reproduced in whole or in part, or stored in a retrieval system, or transmitted in any form (electronic, mechanical, photocopying or otherwise), only with the prior written permission of All SAMOSA project partners*

## 4 SAMOSA SAR ocean retracker performance

### 4.1 Range retrieval accuracy in LRM, RDSAR and SAR mode with the SAMOSA1 SAR ocean retracker from simulated Cryosat data (NOC)

Simulated CryoSat data were provided to the SAMOSA team by the Agency in the form of SARM FBR, SARM L1B and LRM L1B 20Hz waveforms from the CryoSat Mission Performance Simulator (CRYMPS). Simulated data were available for three open ocean scenarios featuring realistic ocean surface waves and variable SWH conditions. The simulated LRM and SARM waveforms were re-tracked with the NOC Brown ocean retracker and the NOC SAMOSA1 ocean retracker respectively. FBR SARM data were reduced to pseudo-LRM waveforms using the RDSAR software developed by STARLAB [CMP2010]. The retracked results for SWH for various scenarios and products are shown in **Figure 5**, with the top row showing the significant wave height conditions in the DEM used as input to the Cryosat simulator. Note that RDSAR pseudo-LRM results are only shown for  $n=8$  in this figure. A similar plot can be produced for retrieved range but is not shown here.

*The copyright in this document is vested in SAMOSA project partners This document may only be reproduced in whole or in part, or stored in a retrieval system, or transmitted in any form (electronic, mechanical, photocopying or otherwise), only with the prior written permission of All SAMOSA project partners*

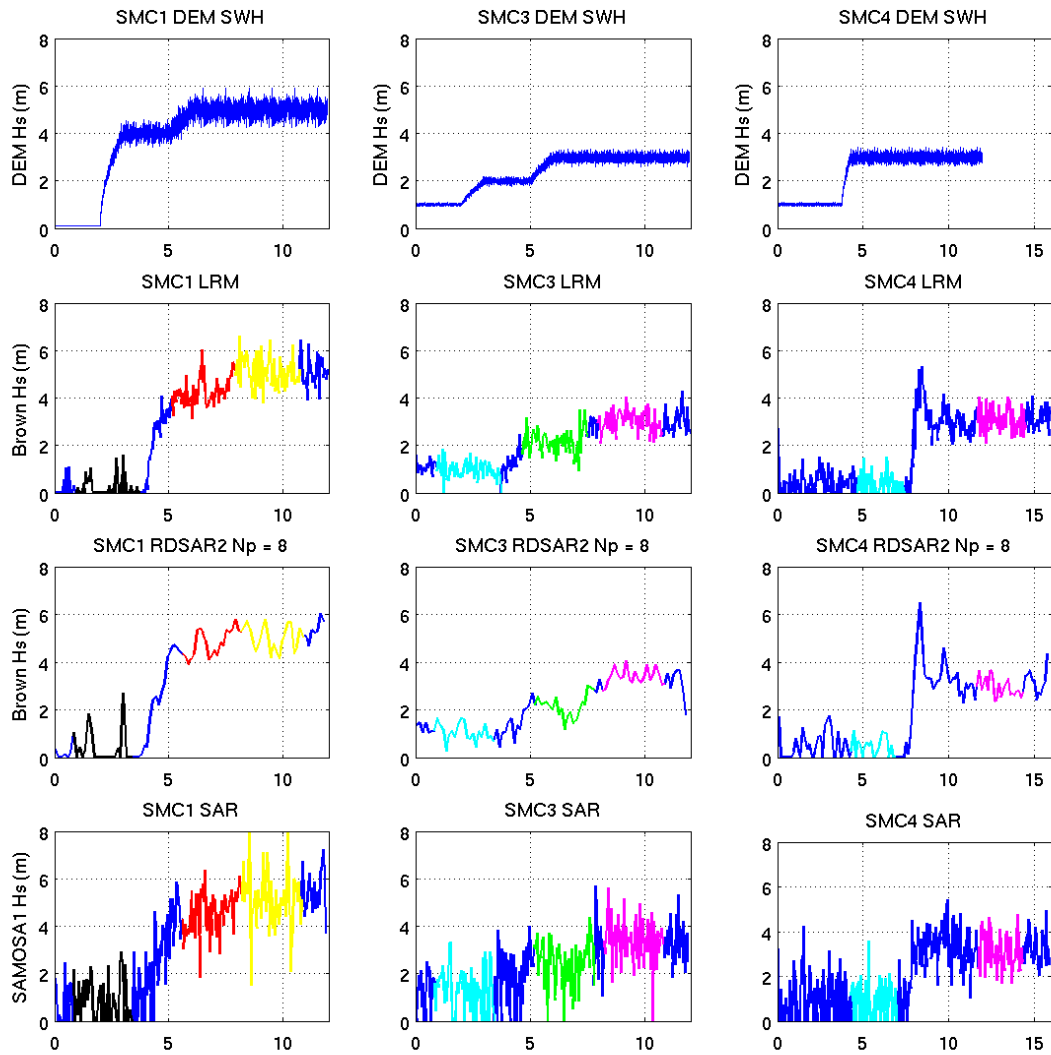


**Figure 5** Simulated DEM SWH (first row) and retracted SWH for LRM (second row), pseudo-LRM (third row) and SARM (fourth row) for the three scenarios over ocean. Colours indicate segments of 2 seconds of data at the same SWH in the DEM. Note that there is a known mis-registration along the x-axis between the DEM (top-row) and the simulated products (rows 2-4).

*The copyright in this document is vested in SAMOSA project partners This document may only be reproduced in whole or in part, or stored in a retrieval system, or transmitted in any form (electronic, mechanical, photocopying or otherwise), only with the prior written permission of All SAMOSA project partners*

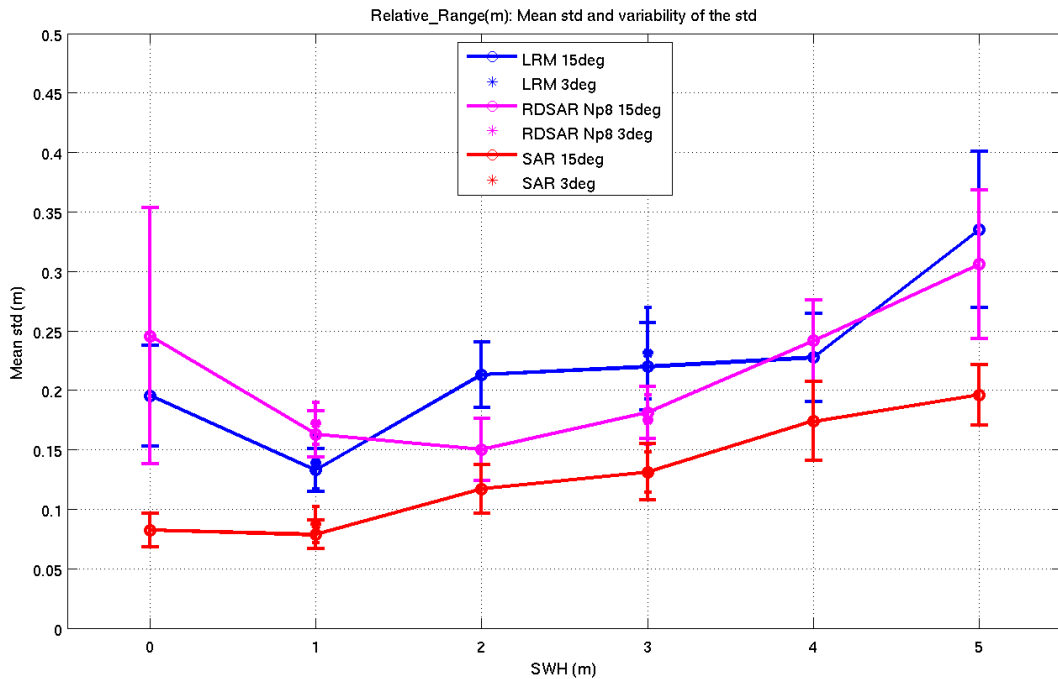


**Figure 6: Range retrieval accuracy as a function of SWH in LRM (blue), pseudo-LRM (magenta) and SARM (red) based on simulated data over ocean.**

Based on these results, it is possible to estimate the retrieval accuracy as a function of SWH. The results for relative range (i.e. the position of the leading edge in the window) are shown in **Figure 6**.

From this we conclude that:

- RDSAR waveforms offer similar performance to those in LRM mode for the retrieval of both SWH and range.
- SAR mode offers an almost two-fold improvement in the retrieval of range.

Based on simulated data, the retrieval accuracy for SWH in SAR mode (not shown) is found to be much worse than for LRM.

## 4.2 Improvement of SAMOSA1 retracker in low wave height conditions (NOC)

The original SAMOSA1 model was known to feature numerical singularities in the waveform trailing edge in low SWH. This resulted in partial data loss in the modelled waveforms and an inability of the SAMOSA1 retracker to return values of SWH smaller than  $\sim 2\text{m}$ .

An analytical solution was investigated, found and implemented to resolve this problem. **Figure 7** illustrates the data loss in the original SAMOSA1 formulation (solid lines), and the improved solution (crosses) in the case of very low wave height. The improved solution has no data loss in late gates, making it possible to use the full gate range to retrack measured waveforms.

The enhanced formulation was implemented in the SAMOSA1 SARM retracker, and applied to SAR waveforms from one of the simulated scenarios (SMC1), which feature very low wave height conditions. This was done side by side with the original SAMOSA1 formulation, to estimate the impact on computation time. The SARM retracked results obtained with the original and the enhanced SAMOSA1 formulations are shown in **Figure 8**. The enhanced formulation leads to improved retrieval of both range and SWH, is now able to return small values of SWH, and results in an almost ten-fold increase in computation speed.

*The copyright in this document is vested in SAMOSA project partners This document may only be reproduced in whole or in part, or stored in a retrieval system, or transmitted in any form (electronic, mechanical, photocopying or otherwise), only with the prior written permission of All SAMOSA project partners*

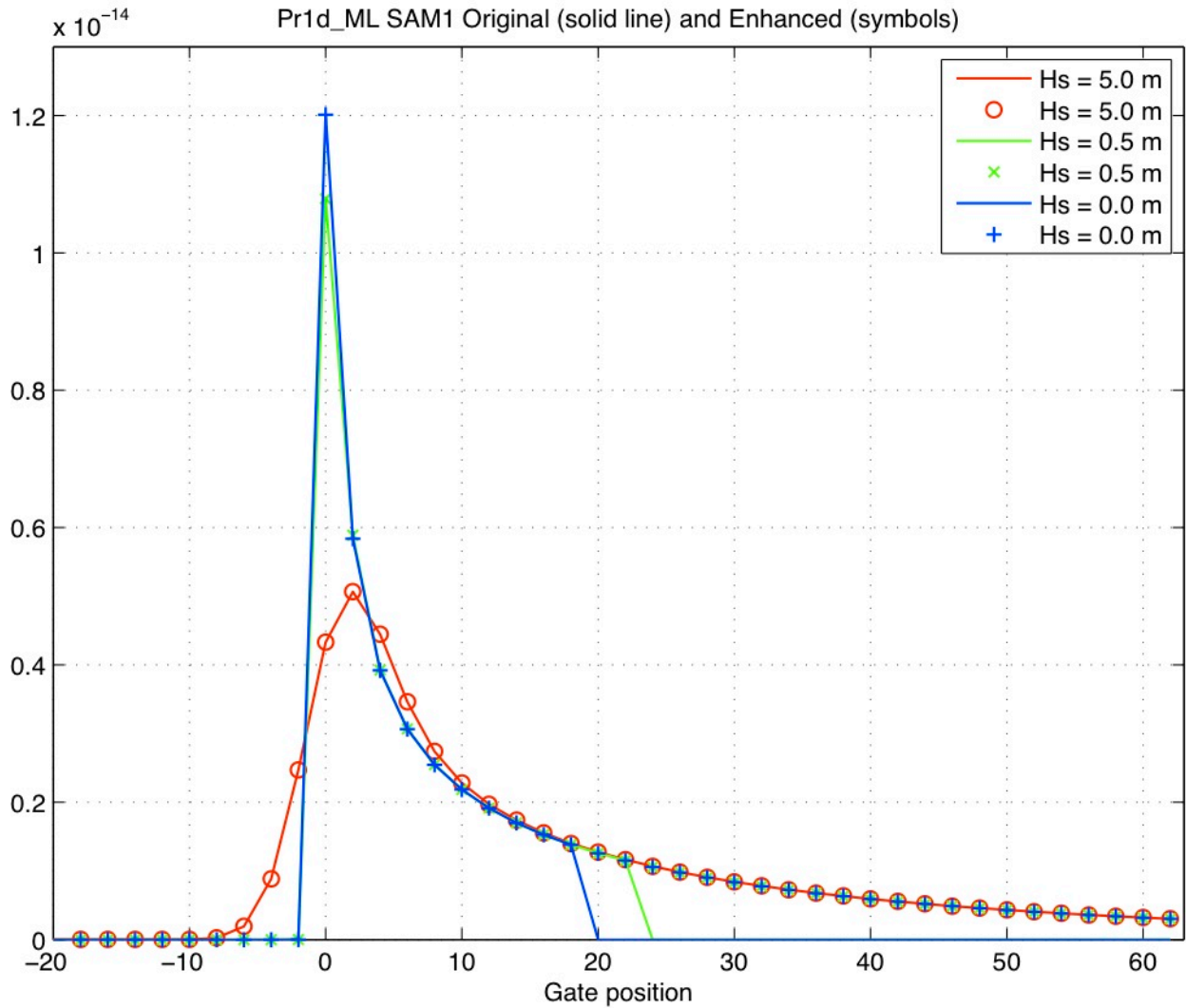


Figure 7: SAMOSA1 Multi-looked waveforms for various SWH conditions for the original formulation (solid line) and the extended analytical solution (crosses). The original formulation displayed data loss in the trailing edge for low significant wave height conditions due to a numerical instability in the original SAMOSA1 model.

The copyright in this document is vested in SAMOSA project partners This document may only be reproduced in whole or in part, or stored in a retrieval system, or transmitted in any form (electronic, mechanical, photocopying or otherwise), only with the prior written permission of All SAMOSA project partners

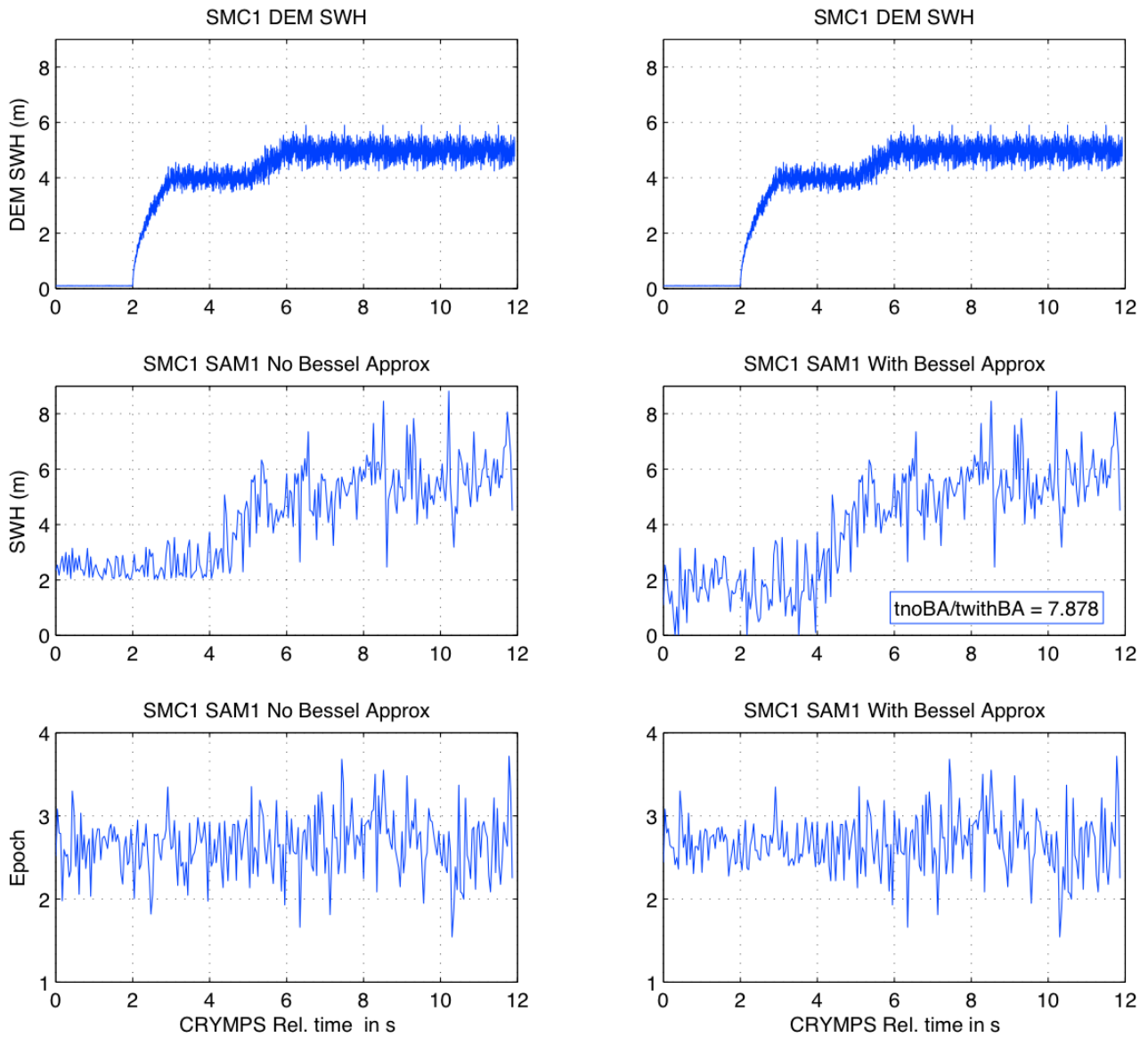
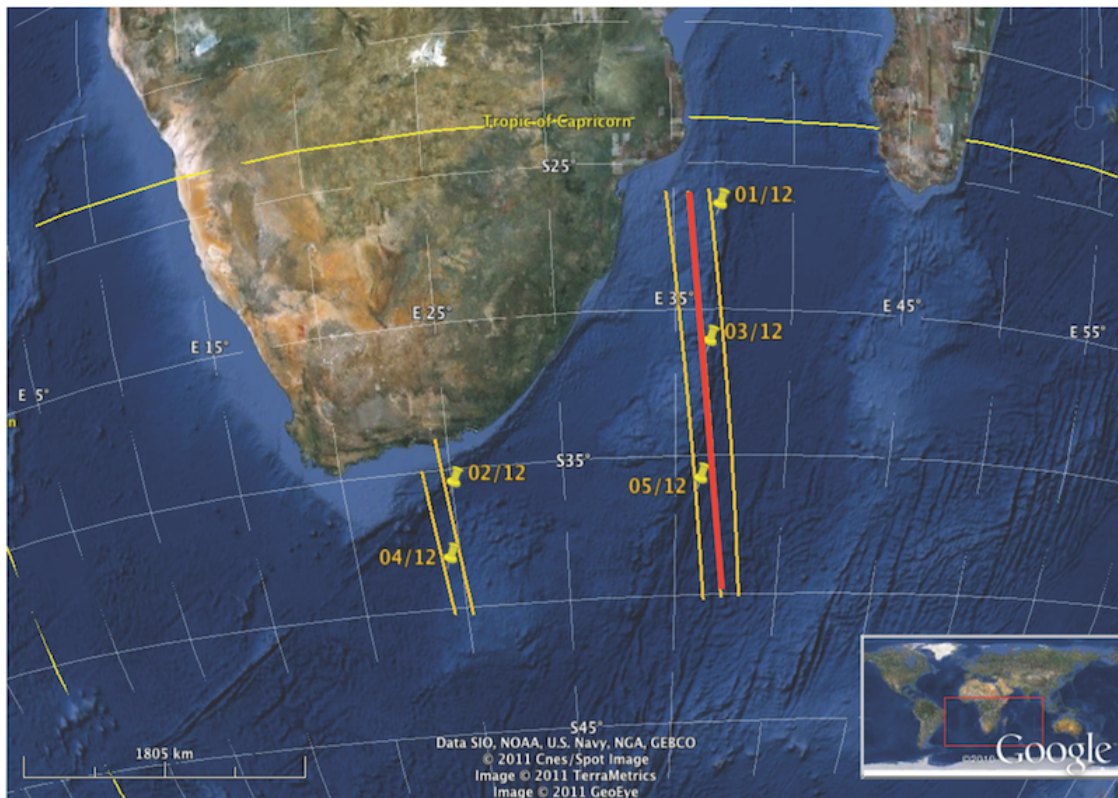


Figure 8: SAMOSA1 SAR retracker results for simulated scenario SMC1 using the (left) original SAMOSA1 model formulation and (right) the improved analytical solution. The analytical solution results in an almost 10-fold increase in computation speed.

### 4.3 Application of the SAMOSA1 retracker to CryoSat-2 SARM data (NOC)

The SAMOSA1 SAR retracker was applied to CryoSat-2 L1B SAR waveform data in some selected locations where CryoSat-2 SARM data is available. **Figure 9** and **Figure 10** show the location and the output of an example of SAR retracking with the SAMOSA1 model applied to Cryosat-2 L1B SAR data over the Agulhas region.

*The copyright in this document is vested in SAMOSA project partners This document may only be reproduced in whole or in part, or stored in a retrieval system, or transmitted in any form (electronic, mechanical, photocopying or otherwise), only with the prior written permission of All SAMOSA project partners*



**Figure 9: L1B SARM data track (in red) over the Agulhas region.**

The results shown in **Figure 10** correspond to a landward ascending pass, with latitude 35 degree signalling the presence of a major ridge on the sea floor (seen in the top and second top panels). The retrieved SAR SWH (third panel) shows a gradual decrease from 5 to 3 metres as one travels northwards, which is consistent with the wave field reported by other altimeters on the same day, although the SAR estimates of SWH appear slightly over-estimated. Both the SAR retrieved SWH and the absolute range anomaly (defined as the satellite\_height minus range shown in the bottom subplot) present variability and features consistent with geophysical signals that one can expect in this region.

In order to revisit the issue of SAR retrieval accuracy in different sea states, the SAMOSA1 retracker was applied to a large number of Cryosat2 L1B SAR products in a small region in the Norwegian Sea. The Cryosat2 data corresponded to acquisitions made between July 2010 and March 2011, thus featuring a wide range of sea states. **Figure 11** shows the retrieved SAR SWH and absolute range anomaly obtained by retracking the Cryosat2 L1B SAR waveforms. The same quantities were estimated for Jason2 LRM data over the same region and the same period, based on AVISO Jason-2 Level 2 products, and these results are shown in **Figure 12**.

Each data segment in **Figure 11** and **Figure 12** corresponds to about 6 seconds of data at 20Hz (~ 120 waveforms). Note that no attempt was made to collocate the two satellites in time, as there are very few cases of crossover time difference less than 6 hours. For each 6-second dataset, the 20Hz retrieval accuracy is estimated for range and SWH as the standard deviation within 1s of data. The results for Cryosat2 SAR and Jason2 LRM are shown as a function of retrieved SWH in Figure 13, where the error bars represents the variability in the 20Hz retrieved accuracy estimated from the 6 seconds of data.

We find that, based on this dataset, the 20Hz retrieval accuracy for range varies between 7-14 cm for Jason2 LRM and between 4-10 cm for Cryosat2 SAR for significant wave height between 1-7 metres. For significant wave height, the 20Hz retrieval accuracy varies between 0.5-0.75 m for Jason2 LRM and between 0.3-0.6 m for Cryosat2 SAR. These results confirm that SAR mode yields a significant improvement in range retrieval accuracy compared to conventional altimetry, as previously suggested by our results based on simulated data. These results also indicate that, contrary to our previous findings with simulated SAR waveforms, the retrieval accuracy of SWH is as good, maybe even slightly better, in SAR mode than in LRM mode.

*The copyright in this document is vested in SAMOSA project partners This document may only be reproduced in whole or in part, or stored in a retrieval system, or transmitted in any form (electronic, mechanical, photocopying or otherwise), only with the prior written permission of All SAMOSA project partners*

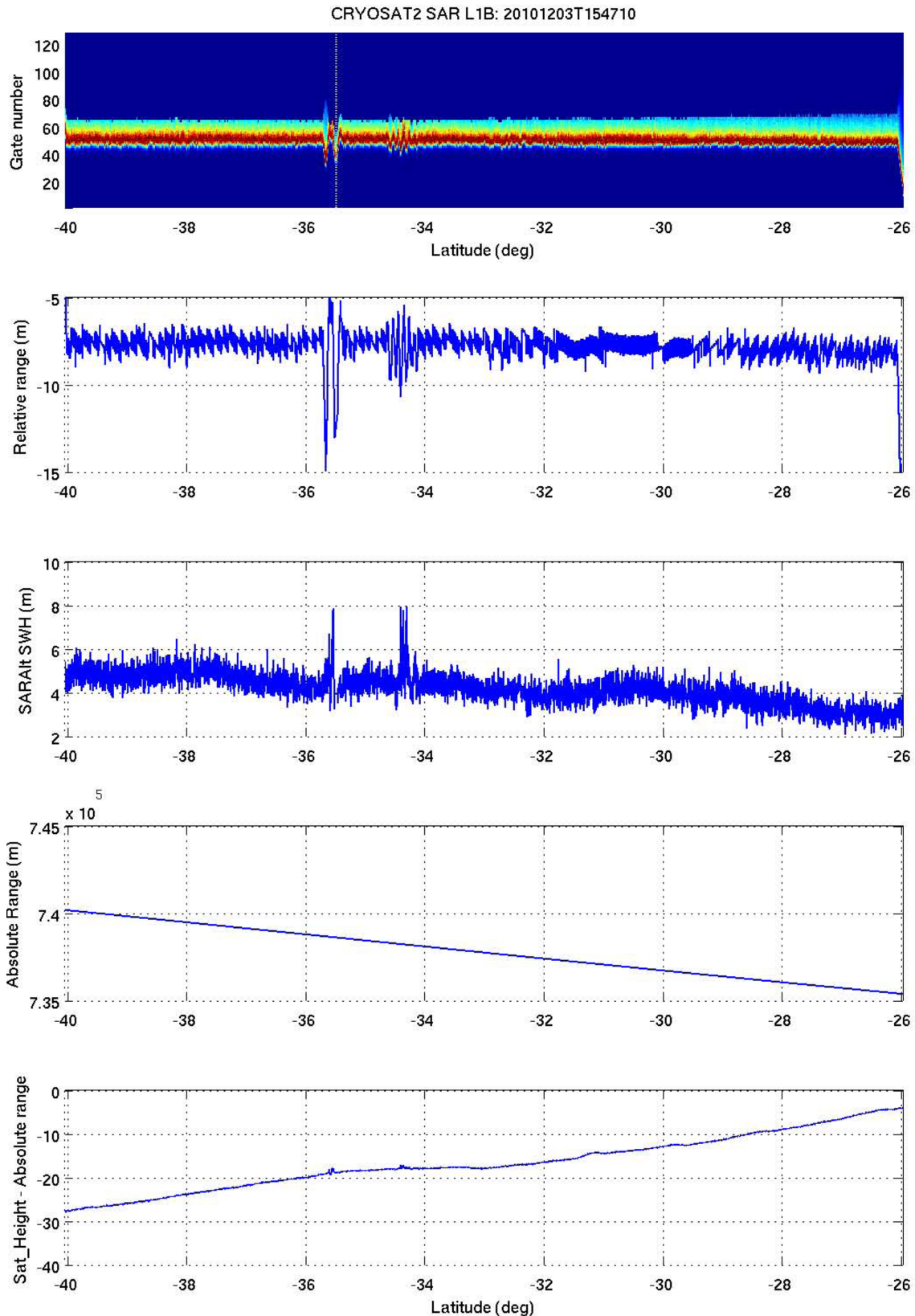


**Figure 10: Retracked SAR results, showing from top to bottom: L1B SAR waveforms; relative range of leading edge within ranging window; retrieved SAR SWH; satellite to surface range; Satellite\_height minus range in metres**

*The copyright in this document is vested in SAMOSA project partners This document may only be reproduced in whole or in part, or stored in a retrieval system, or transmitted in any form (electronic, mechanical, photocopying or otherwise), only with the prior written permission of All SAMOSA project partners*

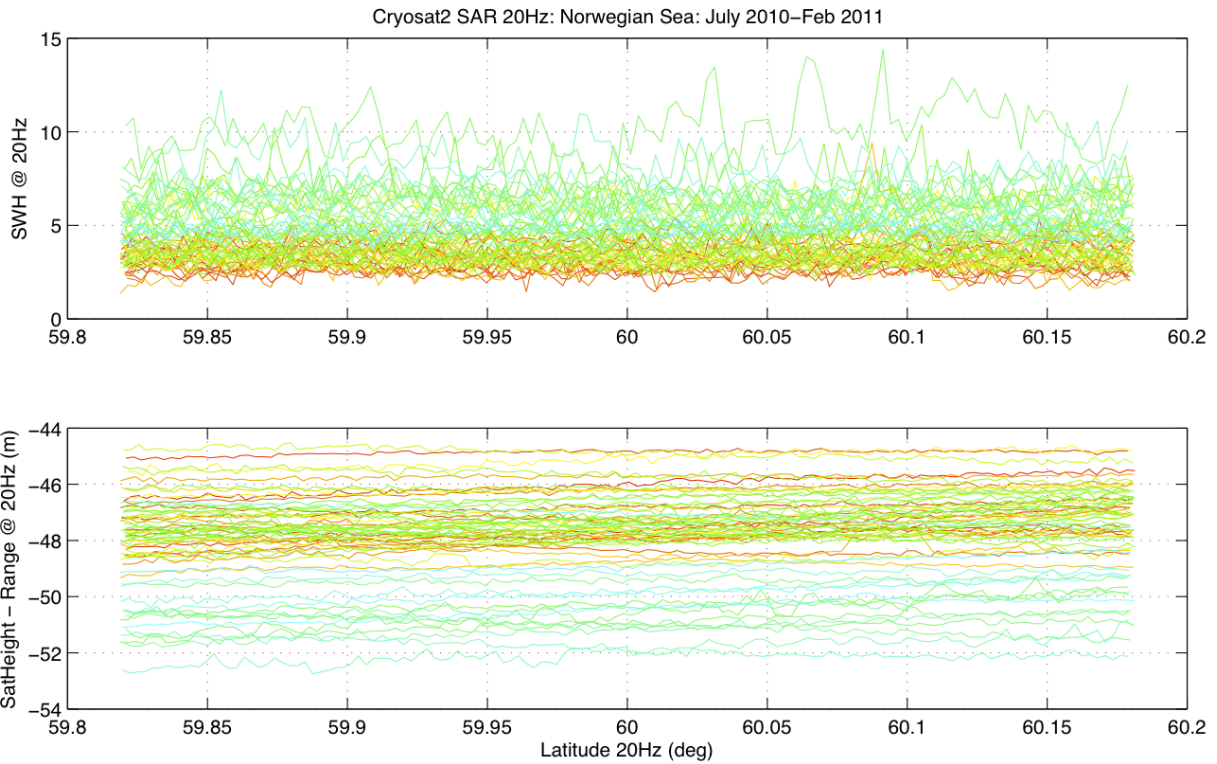


**Figure 11: Retrieved SAMOSA1 SWH and absolute range anomaly for Cryosat2 L1B SAR data over a small region of the Norwegian Sea between July 2010 and March 2011.**

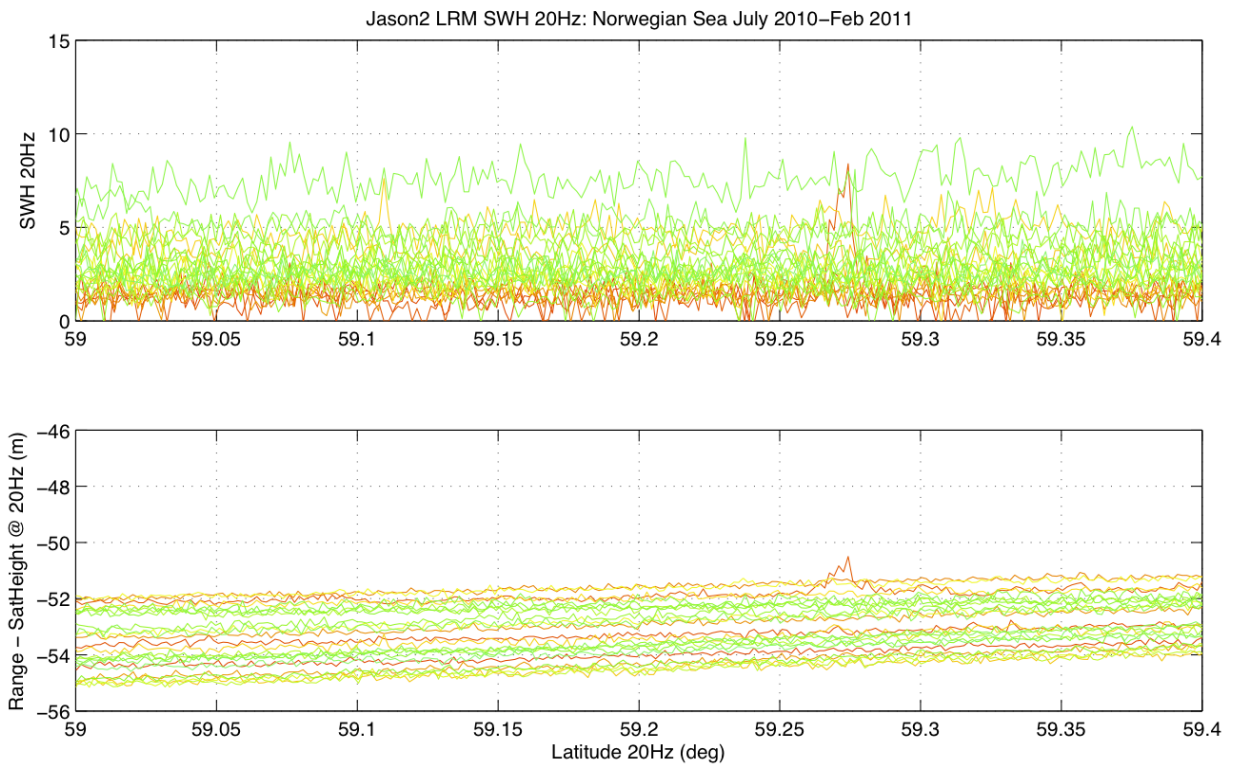


**Figure 12: Retrieved SAMOSA1 SWH absolute range anomaly for Jason2 LRM data over small region of the Norwegian sea between July 2010 and March 2011.**

*The copyright in this document is vested in SAMOSA project partners This document may only be reproduced in whole or in part, or stored in a retrieval system, or transmitted in any form (electronic, mechanical, photocopying or otherwise), only with the prior written permission of All SAMOSA project partners*

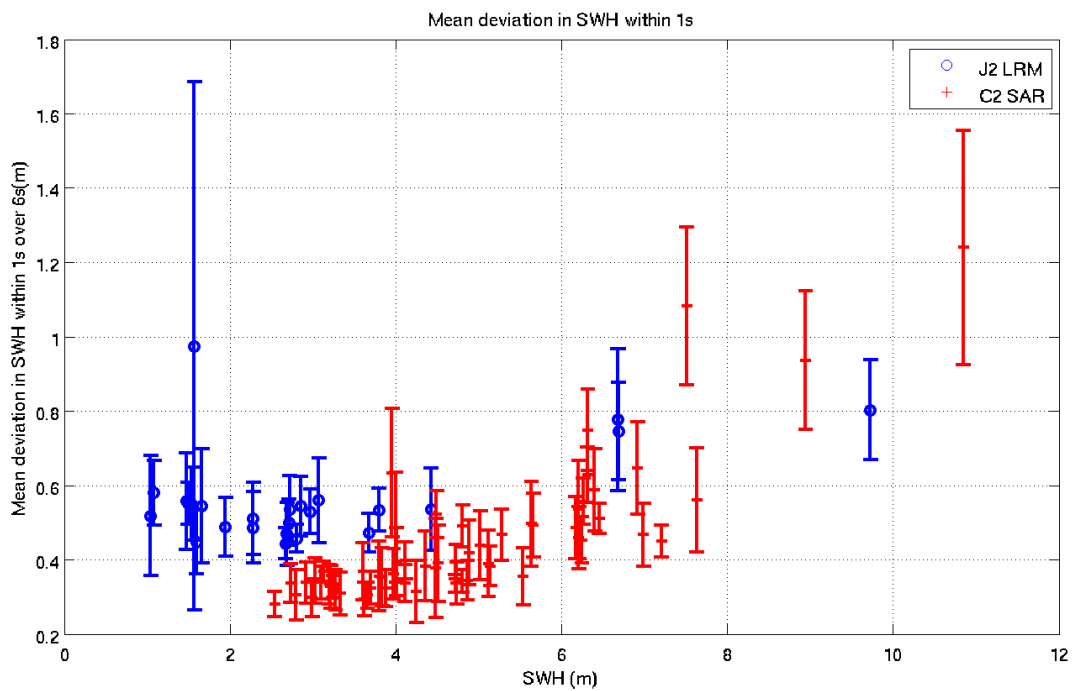
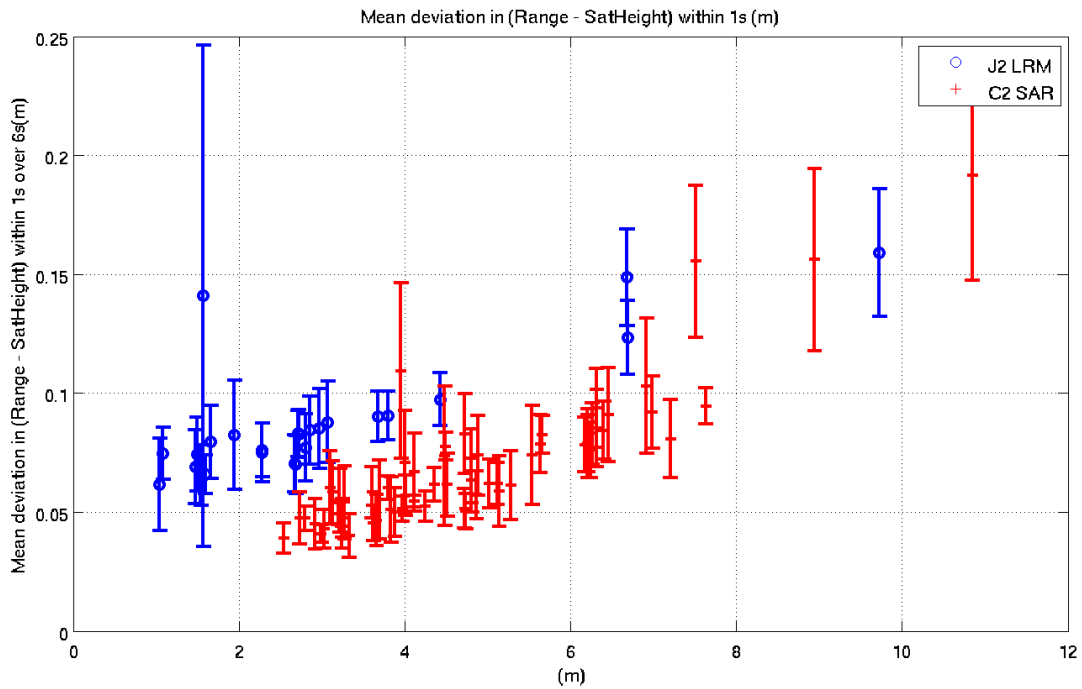


Figure 13: Retrieval accuracy at 20Hz for SWH (top) and absolute range anomaly (bottom) as a function of Significant Wave Height for Jason-2 LRM (blue) and Cryosat-2 SAR (red) for data in a small region of the Norwegian Sea between July 2010 and March 2011. The Cryosat-2 SAR data were retracked with the SAMOSA1 Extended model.

The copyright in this document is vested in SAMOSA project partners This document may only be reproduced in whole or in part, or stored in a retrieval system, or transmitted in any form (electronic, mechanical, photocopying or otherwise), only with the prior written permission of All SAMOSA project partners

#### 4.4 SAMOSA1 retracker performance with ASIRAS data (DTU)

The ASIRAS instrument was developed under the ESA technology research program for calibration and validation of the CryoSat measurements. To ensure reliable data collection over steep and rapid varying terrain it was decided to use an antenna with an along-track 3 dB beam width of  $10^\circ$ , with an across-track 3 dB beam width of  $2.5^\circ$  and a highly elliptical antenna gain pattern. Due to the wide along-track beam width, ASIRAS typically operates at a pulse repetition frequency of 2.5 kHz to ensure an unambiguous sampling of the Doppler spectrum [MAV2004]. The short two-way travel time associated with the ASIRAS instrument allows each radar pulse to be received before the next pulse is emitted, while maintaining a PRF high enough to allow SAR processing.

Airborne ASIRAS data acquired on April 30 2006 between 10:08:49 and 10:23:05 UTC, covering a profile from  $77^\circ 57' 02.38''$  N,  $4^\circ 39' 41.85''$  W to  $78^\circ 05' 29.21''$  N,  $2^\circ 08' 21.05''$  W in the Fram Strait between Greenland and Svalbard [STE2007], has been processed from L0 to L1b using the ASIRAS processor [CUL2010] and a set of processing schemes.

A retracker based on the SAMOSA1 waveform model has been adapted to accommodate the parameters for the ASIRAS instrument and applied on the L1b ASIRAS data. Finally the output of the retracker has been validated against the DTU10 Mean Sea Surface [AND2009] and the ECMWF wave model [ABD2011].

When the along-track look angle increases beyond a certain threshold, the look will no longer contribute positively to the averaged waveform and should therefore be rejected during post-processing. The standard ASIRAS processing scheme uses a maximal along-track look angles of  $6^\circ$ , however investigations show that, for this profile, a maximal along-track look angle of  $1.4^\circ$  is a good compromise between a high number of looks and a low look angle [STE2009]. Due to the short two-way travel time the number of pulses in a burst can be decided during post-processing. Burst sizes of 64, 128, and 256 pulses, corresponding to along-track footprint sizes of 16.69 m, 8.34 m, and 4.17m, have been combined with maximal along-track look angles of  $1.4^\circ$  and  $6^\circ$  to form a number of processing schemes [STE2011].

The SAMOSA1 retracker has been applied on the L1b output of the ASIRAS processor for each of the processing runs and the ASIRAS instrument range correction has been applied. The overall best result was obtained using a processing scheme with a burst size of 64 pulses and a maximal look angle of  $1.4^\circ$  [STE2011]. For this processor run the retracker obtained a successful fit for more than 96% of the waveforms.

**Figure 14** shows an example of an ASIRAS waveform on the fitted SAMOSA1 waveform. It is noted that the SAMOSA1 retracker does not capture the rapid decaying trailing edge in the ASIRAS data. This is believed to be related to the fact that the across-track footprint for the ASIRAS profile is beam limited and not pulse limited as assumed in the SAMOSA1 waveform model. For the profile the average range to the surface is 2734 m resulting in an across-track beam limited footprint of approximately 120 m. For the ASIRAS profile used, the across-track footprint would be pulse limited only when the significant wave height is below 0.56 m.

The surface height obtained is shown in **Figure 15** and the significant wave height is shown in **Figure 16** or the entire profile. From **Figure 15** and **Figure 16** it is seen that the retracker is performing stably and gives consistent results, when areas with large aircraft manoeuvres (e.g. at  $-4.6^\circ$  and  $-2.4^\circ$  longitude) are excluded. Data outside  $-4.5^\circ$  to  $-2.5^\circ$  longitude are excluded due to large aircraft manoeuvres that are known to degrade the data. The average and the standard deviation are calculated for the remaining data.

The average surface height is found to be 39.63 m with a standard deviation of 0.36 m. This is in agreement with the 40.71 m estimated with the DTU10 Mean Sea Surface [AND2009], when considering that the data has not been corrected for tide or inverse barometric effect.

The significant wave height is found to be 0.93 m with a standard deviation of 0.40 m. From the ECMWF wave model the significant wave height is predicted to be 1.83 m at 06:00 UTC and 1.46 m at 12:00 UTC [ABD2011] which is higher than the significant wave height determined by the retracker. The lower significant wave height is likely to be caused by the profile data being across-track beam limited.

It can be concluded that overall the SAMOSA1 retracker is found to perform well with ASIRAS data when

*The copyright in this document is vested in SAMOSA project partners This document may only be reproduced in whole or in part, or stored in a retrieval system, or transmitted in any form (electronic, mechanical, photocopying or otherwise), only with the prior written permission of All SAMOSA project partners*

choosing an appropriate processing scheme and acknowledging the fundamental differences between air- and space-borne systems.

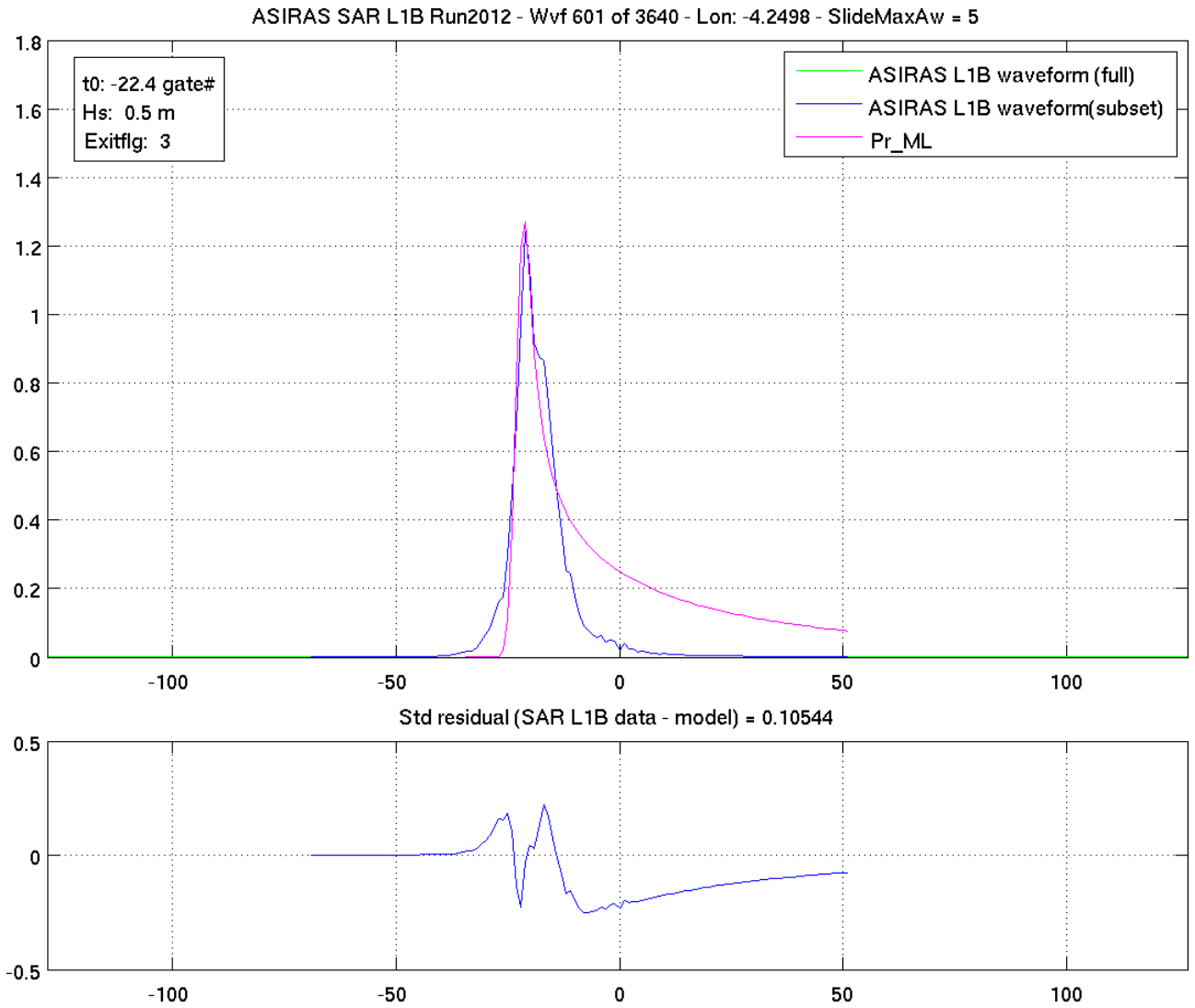


Figure 14: Example of ASIRAS waveform (blue) and fitted SAMOSA1 waveform (pink)

*The copyright in this document is vested in SAMOSA project partners This document may only be reproduced in whole or in part, or stored in a retrieval system, or transmitted in any form (electronic, mechanical, photocopying or otherwise), only with the prior written permission of All SAMOSA project partners*

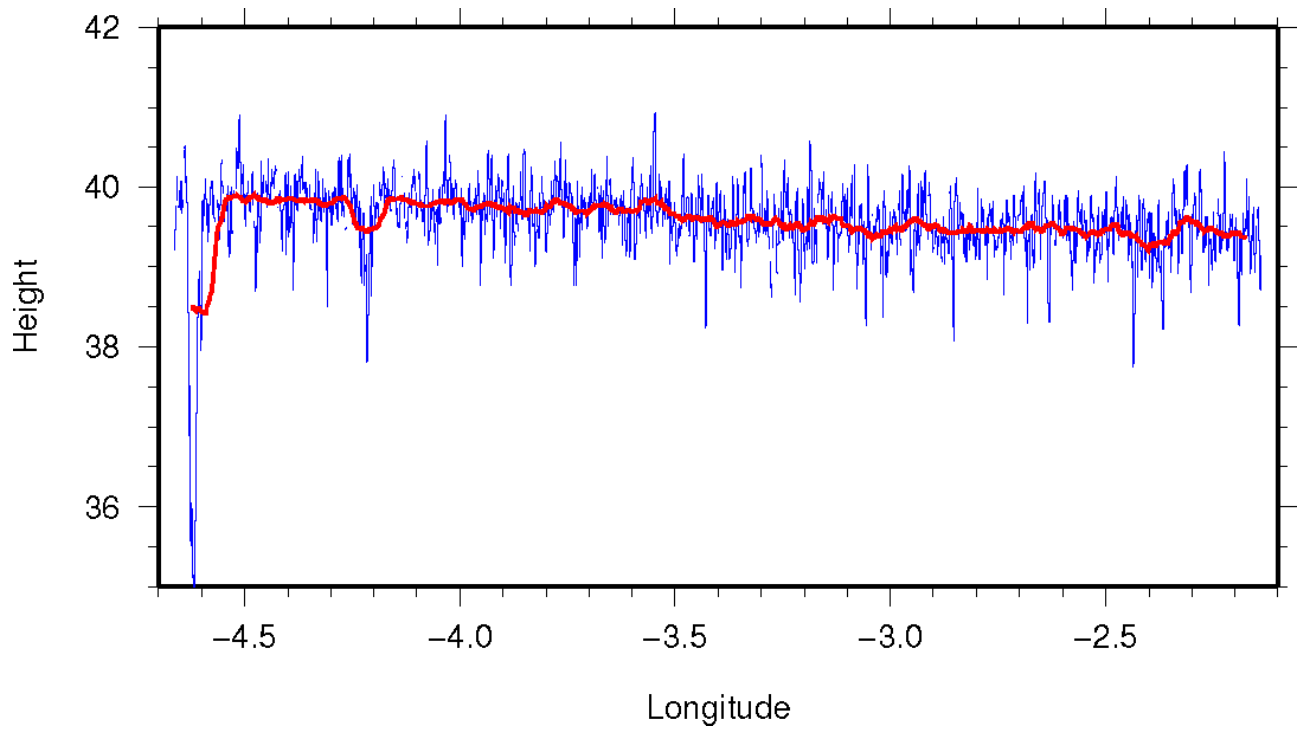


Figure 15: Estimated surface elevation (blue) and 100 samples running average (red).

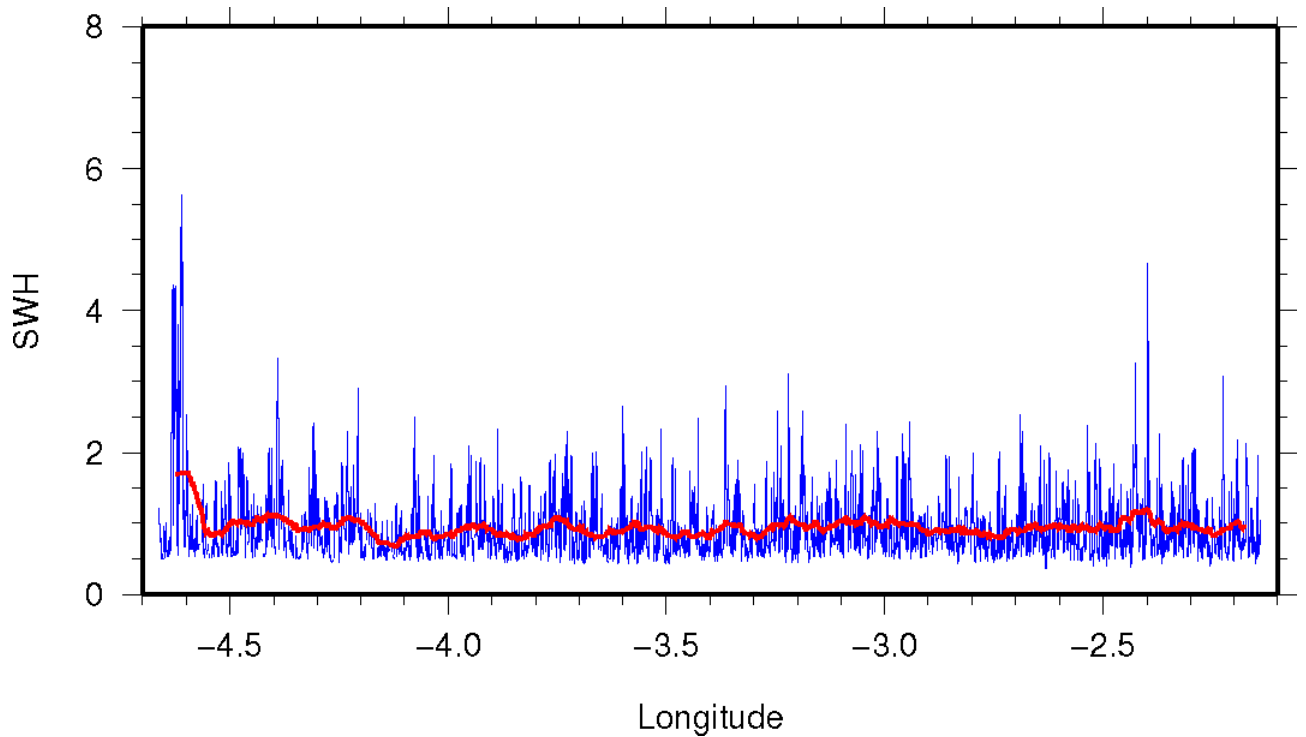


Figure 16: Estimated SWH along the profile (blue) and 100 samples running average (red).

*The copyright in this document is vested in SAMOSA project partners. This document may only be reproduced in whole or in part, or stored in a retrieval system, or transmitted in any form (electronic, mechanical, photocopying or otherwise), only with the prior written permission of All SAMOSA project partners.*

## 4.5 Implementation of the SAMOSA2 model as a SAR ocean retracker and mispointing effects (NOC)

The SAMOSA2 model was derived by STARLAB [RAY2011] and implemented by NOC in the SAMOSA2 SAR ocean retracker. The SAMOSA2 model is a completely new formulation, much more complex than SAMOSA1. Among others features, SAMOSA2 can account for non-linear ocean wave statistics and deals more accurately with the effect of mispointing on SAR waveforms. The effect of along-track mispointing on the single-look delay-Doppler maps is shown in **Figure 17**. Very large values of mispointing result in a significant loss of power, a widening of the waveforms and a change in the position of the leading edge.

SAMOSA2 Single-look Delay Doppler Map: lat0 = 45deg; t0 = 0; Hs = 3m

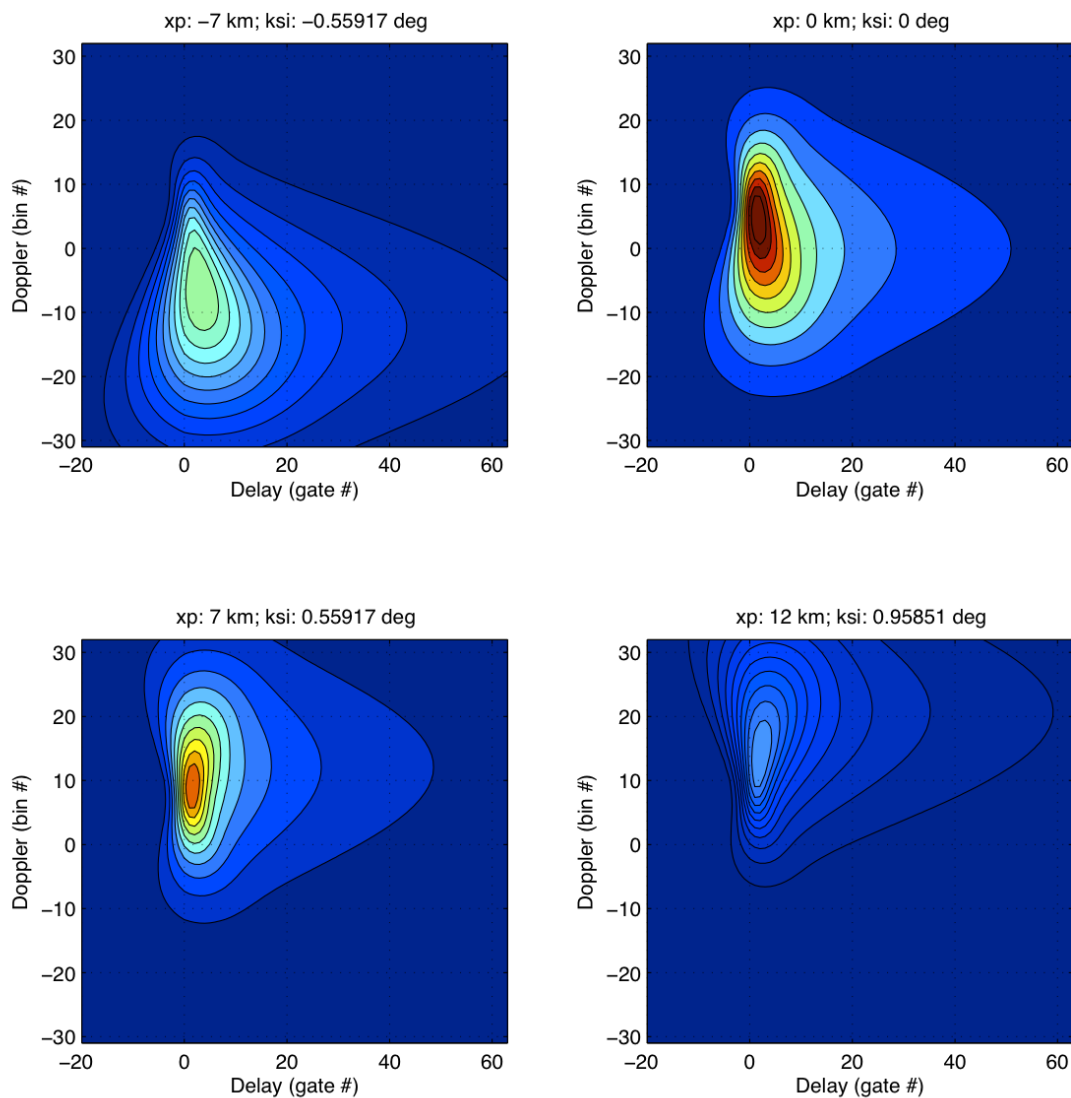


**Figure 17: SAMOSA2 Single-look Delay Doppler maps for SWH = 3m, latitude = 45° and various values of along track mispointing. showing the effect of mispointing on the power distribution in the DDM and on the power returns. All subplots use the same colour scale. ksi represents the mispointing angle from the nadir in the along-track direction while x\_p stands for the associated along-track displacement on the ground of the antenna centre due to the mispointing.**

*The copyright in this document is vested in SAMOSA project partners This document may only be reproduced in whole or in part, or stored in a retrieval system, or transmitted in any form (electronic, mechanical, photocopying or otherwise), only with the prior written permission of All SAMOSA project partners*

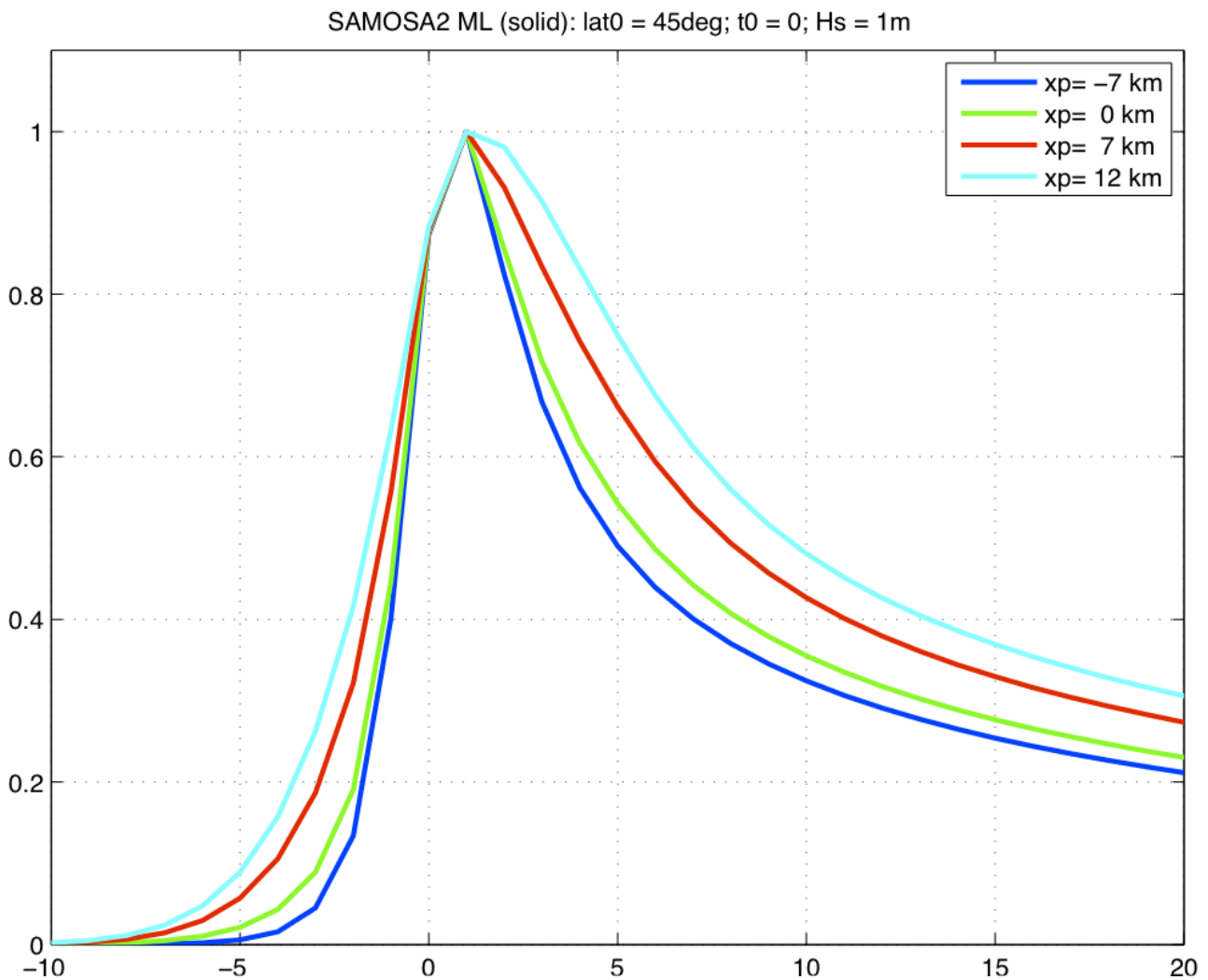


**Figure 18: SAMOSA2 Single-look Delay Doppler maps for SWH = 1m, latitude = 45° and various values of along track mispointing.  $x_p$  stands for the associated along-track displacement on the ground of the antenna centre due to the mispointing. An  $x_p$  value of 7 km corresponds to an angular mispointing of approximately 0.6°**

The SAMOSA2 model is considerably slower to compute because of its dependence on some quadrature terms. In its linear form, the SAMOSA2 model is about 300 times slower than the SAMOSA1 model.

Analytical solutions for the SAMOSA2 quadrature terms ( $f_0$ ,  $f_1$ ) have been investigated and found. A computationally efficient solution was implemented for  $f_0$ , resulting in halving of the processing time. However, finding a computational efficient way to calculate the analytical solution to  $f_1$  remains work in progress.

#### 4.6 Range retrieval accuracy in LRM and SAR mode from computer simulations with the SAMOSA2 retracker (NOC)

Two additional datasets of simulated Cryosat L1B waveforms were obtained over ocean to investigate the performance of the SAMOSA2 retracker in the presence of mispointing. The two new simulated runs correspond to the same SWH conditions as used previously in scenario SMC3, i.e. with SWH changing from 1 to 2 to 3 meters. Results are presented in **Figure 19** and **Figure 20**. Run S3U7 corresponds to mispointing equal to zero, while run S3U9 corresponds to along-track mispointing equal to 0.05 deg.

*The copyright in this document is vested in SAMOSA project partners This document may only be reproduced in whole or in part, or stored in a retrieval system, or transmitted in any form (electronic, mechanical, photocopying or otherwise), only with the prior written permission of All SAMOSA project partners*

**Figure 19** shows multi-looked SAR waveforms in the absence of mispointing for different SWH conditions from the simulated Cryosat SAR product in scenario S3U7 (thick line), the SAMOSA1 model (dashed line) and the SAMOSA2 model (thin line) computed for the same SWH conditions. The SAMOSA models were not fitted to the simulated Cryosat waveforms. These plots therefore illustrate the very good match between the SAMOSA theoretical models and the simulated Cryosat L1B SAR waveforms.

The simulated Cryosat SAR waveforms were retracked with the SAMOSA1 and SAMOSA2 models, with and without mispointing retrieval. The retrieved relative range (position of the leading edge within the ranging window) is shown in **Figure 20** for various combinations of models and products. Results for scenario S3U7 (no mispointing) are shown on the left, and on the right for scenario S3U9 (mispointing = 0.05 deg). The top row represents the wave height conditions in the DEM used as input to the Cryosat simulator, while row 2 corresponds to the Brown retracker output for simulated LRM data. Rows 3-6 show the relative range obtained by retracking the simulated SARM data respectively with the: SAMOSA1 retracker without mispointing (3 param); SAMOSA1 retracker with mispointing (4 param); SAMOSA2 retracker without mispointing (3 param); SAMOSA2 retracker with mispointing (4 param). As before, the different colours indicate 2 seconds data segments corresponding to the same SWH conditions in the DEM.

From this, the range retrieval accuracy was estimated as before for different SWH conditions, and is reported in **Figure 21**. This confirms the earlier results with simulated data, that range retrieval accuracy in SAR mode results in about a factor of two better than for LRM. There are however large unexplained features in the simulated waveforms that make this a less robust finding.

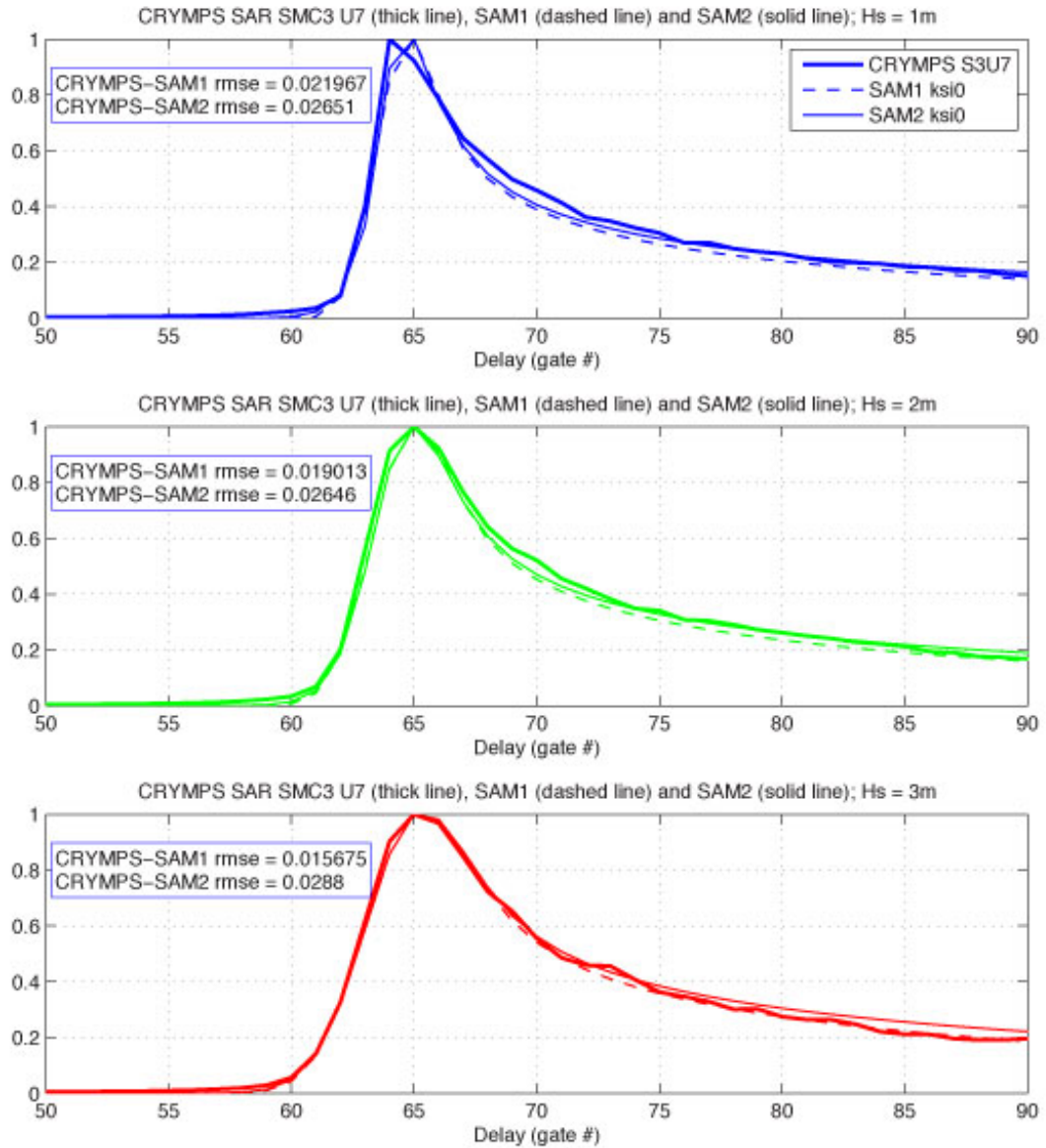
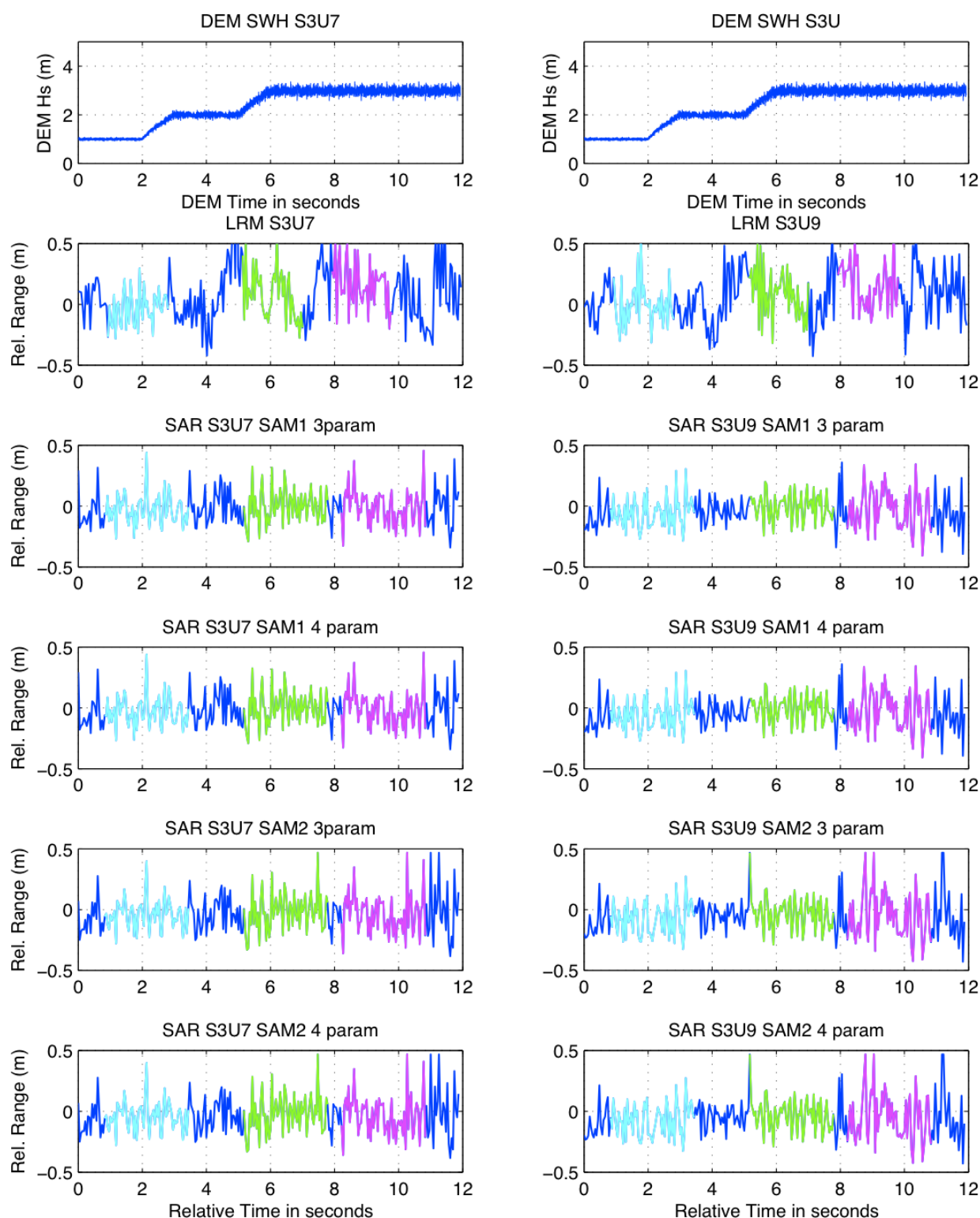


Figure 19: Multi-looked SAR waveforms in the absence of mispointing for SWH equal to 1m (top), 2m (middle), and 3m (bottom) for simulated Cryosat L1B SAR data from S3U7 scenario (1s-average; thick line), SAMOSA1 model (dashed line) and the SAMOSA2 model (thin line). Note that the SAMOSA model waveforms were not fitted to the simulated waveforms.

*The copyright in this document is vested in SAMOSA project partners This document may only be reproduced in whole or in part, or stored in a retrieval system, or transmitted in any form (electronic, mechanical, photocopying or otherwise), only with the prior written permission of All SAMOSA project partners*



**Figure 20: Relative range retrieved from simulated Cryosat products for scenarios S3U7 (left) and S3U9 (right). The top row shows the SWH in the DEM used as input to the Cryosat simulator, while row 2 shows the retrieved range for simulated LRM waveforms retracked with a Brown-type model. Rows 3-6 show the retracked range with the SAMOSA1 and SAMOSA2 SAR waveform models without (3 parameters) and with (4 parameters) mispointing retrieval. Colours indicate segments of 2 seconds of data at the same SWH in the DEM. Note that there is a known mis-registration along the x-axis between the DEM (top row) and the simulated products (rows 2-6).**

*The copyright in this document is vested in SAMOSA project partners This document may only be reproduced in whole or in part, or stored in a retrieval system, or transmitted in any form (electronic, mechanical, photocopying or otherwise), only with the prior written permission of All SAMOSA project partners*

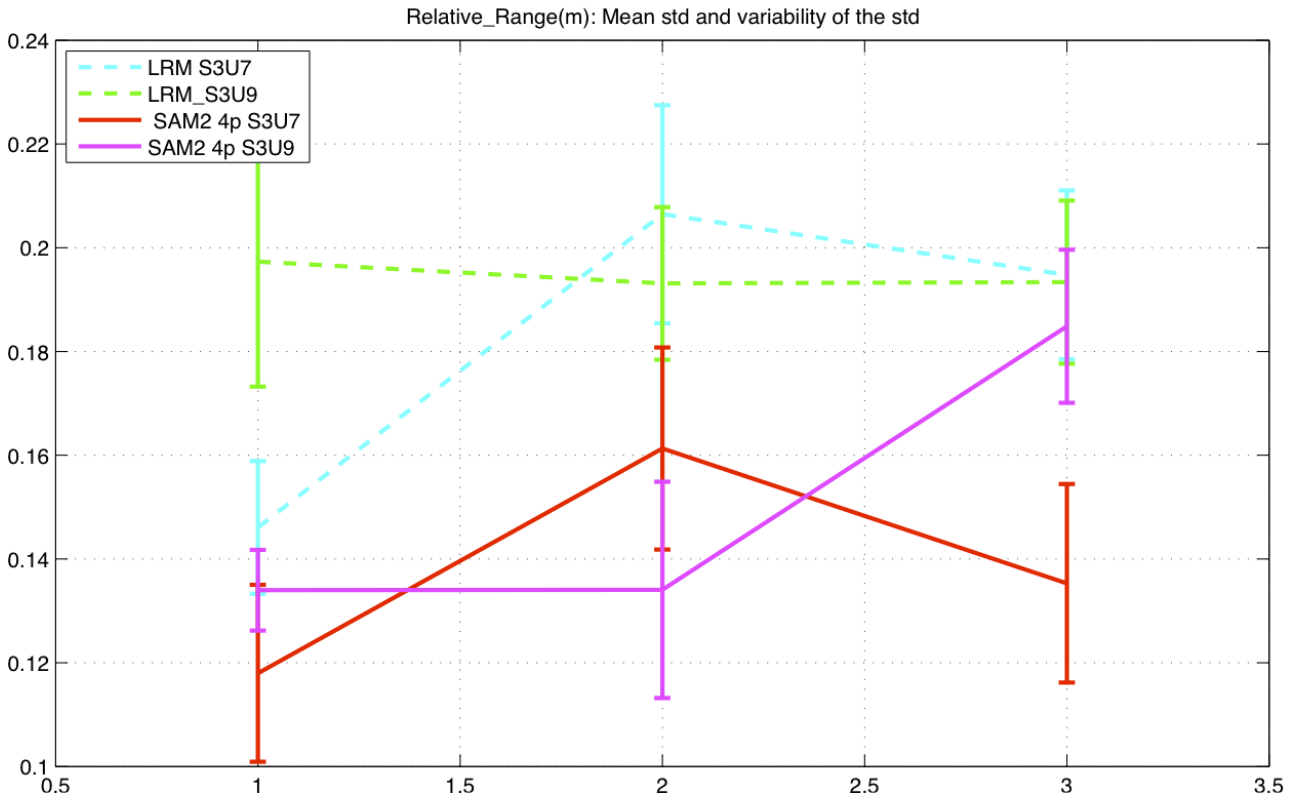


**Figure 21: Range retrieval accuracy (in m) as a function of SWH for LRM (dashed lines) and SAMOSA2 model with mispointing retrieval (solid lines). The results are based on simulated Cryosat data for scenarios S3U7 (cyan/red; no mispointing) and S3U9 (green/magenta; mispointing = 0.05°).**

### 4.7 Application of the SAMOSA2 retracker to CryoSat-2 SAR data (NOC)

The SAMOSA2 SAR retracker has been applied to a small number of CryoSat-2 L1B SAR waveforms but this has been hampered by the much longer processing time needed to compute the SAMOSA2 SAR waveforms with the model in its present form. It is therefore not possible to present extensive retracking results of CryoSat-2 waveforms with the SAMOSA2 model at present. Analytical solutions to speed up the computation of the SAMOSA2 model have been identified and it is simply a matter of time and resources to devise a more efficient software implementation that can be applied to the CryoSat-2 data. In future, we recommend that both SAMOSA1 and SAMOSA2 SAR retrackers should be applied to Cryosat2 data and evaluated by validating their output against independent data source (e.g. Jason-2, wave buoy data).

*The copyright in this document is vested in SAMOSA project partners This document may only be reproduced in whole or in part, or stored in a retrieval system, or transmitted in any form (electronic, mechanical, photocopying or otherwise), only with the prior written permission of All SAMOSA project partners*

## 5 SARM altimetry over in land waters (DMU)

This part of the SAMOSA work was undertaken to assess what information might be retrieved using the CryoSat-2 altimeter over inland water, by preparing inputs for, and analysing output waveforms from, computer simulations. Initially, a generalized scenario was prepared for the Amazon basin, to create a baseline for further work. This contained a generalized topographic model and simplified sigma0 model, with the river system sigma0 values set using ERS1/2 altimeter data. Throughout this work, ERS1, ERS2 and EnviSat sigma0 values were cross-calibrated using previously determined offsets for the different missions and modes.

Simulated output waveforms were obtained, and the SAR L1B dataset was processed through a version of the Berry Expert SysTem (BEST), and successfully retracked. BEST has been developed at DMU and has been slightly modified in the framework of the SAMOSA contract. This crucial baseline analysis informed the second and more detailed case study prepared for part of the Northern U.S.A. Here, the input model complexity was ramped up, especially in the DEM component, using a real dataset supersampled to the spatial resolution required by the simulator from the 1" SRTM DEM available for the USA (**Figure 22**). The backscatter model (**Figure 23**) was synthesised from ERS1 Geodetic Mission data for the longer frequency components, fused with modelled lake components of varying brightness and complexity, with high spatial frequency components added from EnviSat Individual Echoes.

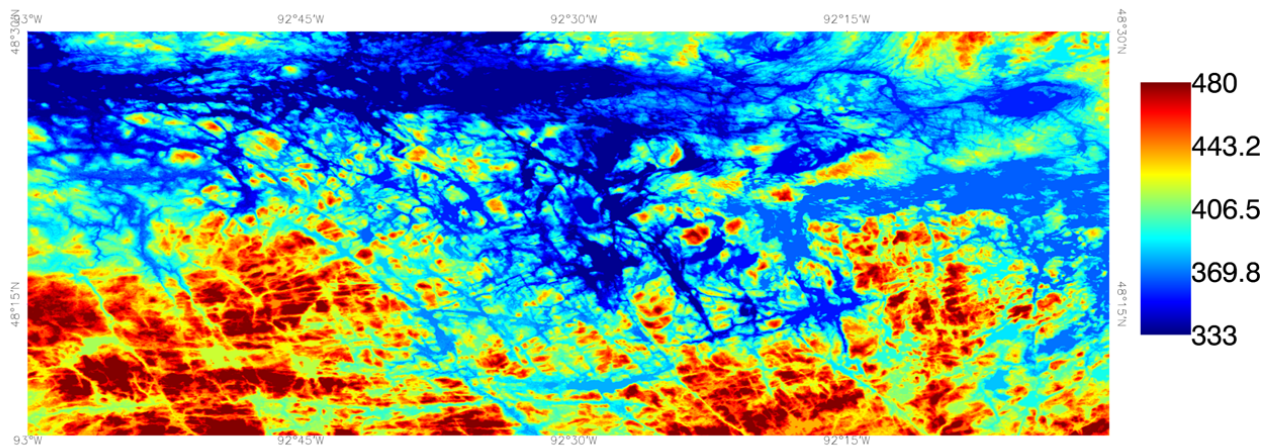


Figure 22: DEM for Lakes Scenario

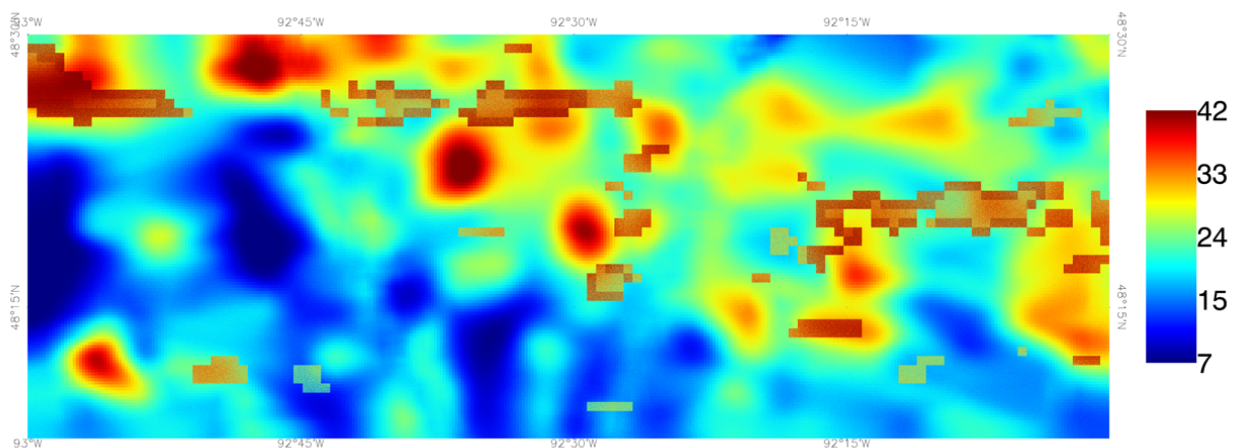
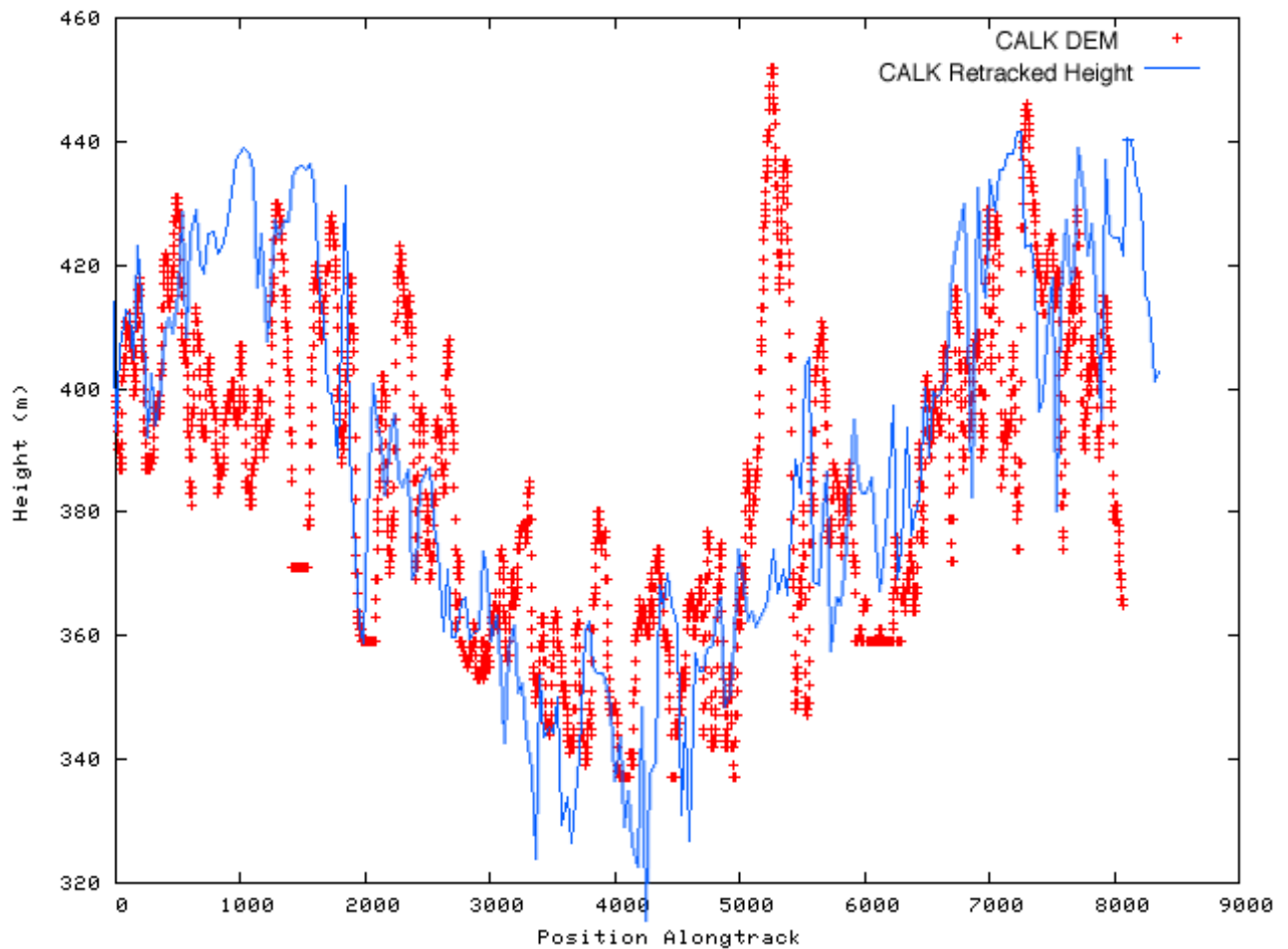


Figure 23: Sigma0 for lakes scenario

*The copyright in this document is vested in SAMOSA project partners This document may only be reproduced in whole or in part, or stored in a retrieval system, or transmitted in any form (electronic, mechanical, photocopying or otherwise), only with the prior written permission of All SAMOSA project partners*

This complex topography stressed the simulator, however data were successfully output from a section of the overpass. The SAR L1B 20Hz data were analysed, and 85% of the waveforms were successfully retracked; **Figure 24** shows the retrieved heights together with the corresponding input DEM heights.



**Figure 24: Retrieved heights from 20Hz SAR waveforms (blue line) with DEM input heights (red crosses)**

One short wavelength topographic peak was not retrieved, but over the more gentle terrain good height recovery was obtained.

A second scenario prepared was for a semi-synthetic estuarine scenario modelled on the Nile delta (**Figure 25**), chosen with less extensive DEM variation to be more easily handled by the simulator. Here, a composite DEM based on ACE2 with high frequency but low magnitude DEM spatial variation was created by 'stamping' the intricately braided channels of the river estuary into the DEM at slightly lower height values. An ocean wave component was added for the coastal sea section of the DEM.

The sigma0 model was formed by reconciling ERS1 GM and ERS2 35 day data to form a background field and introducing higher but variable values for the river channels (**Figure 25**). The 20Hz SAR L1B data were retracked successfully (98% of input waveforms). The output heights from the SAR 20Hz run are shown in **Figure 26**. Sets of 16 SAR FBR waveforms were then stacked and filtered in the frequency domain and the resulting waveforms were analysed. 75% of these waveforms were successfully retracked.

*The copyright in this document is vested in SAMOSA project partners This document may only be reproduced in whole or in part, or stored in a retrieval system, or transmitted in any form (electronic, mechanical, photocopying or otherwise), only with the prior written permission of All SAMOSA project partners*

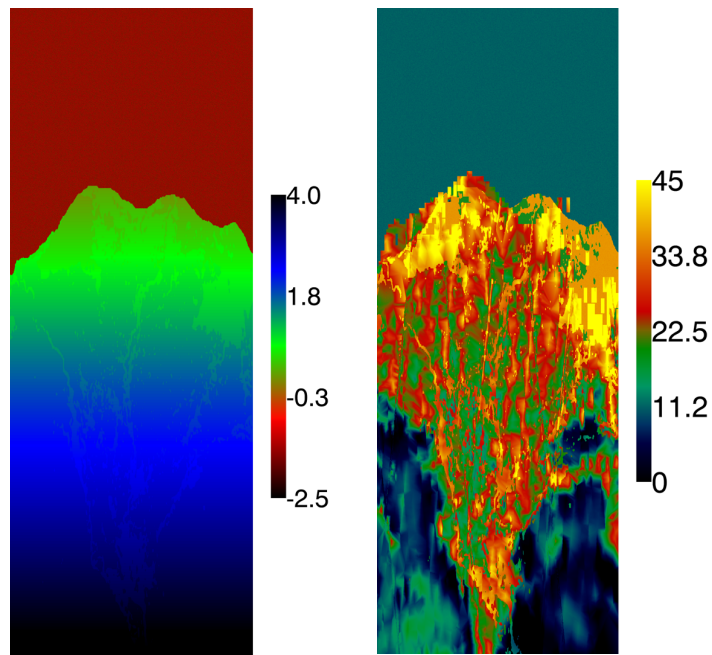


Figure 25: Model inputs for estuarine scenario: DEM (left) and sigma0 (right)

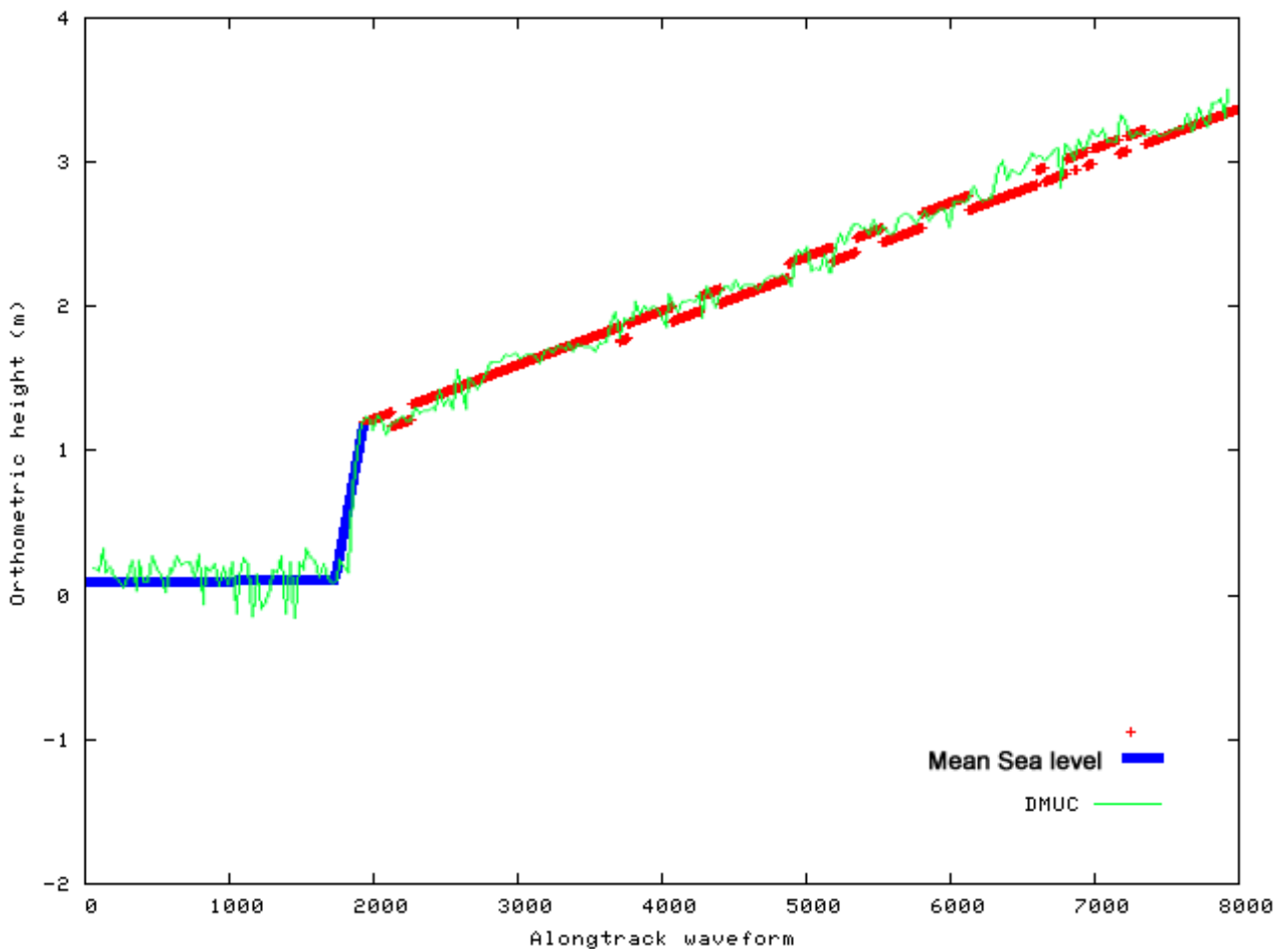
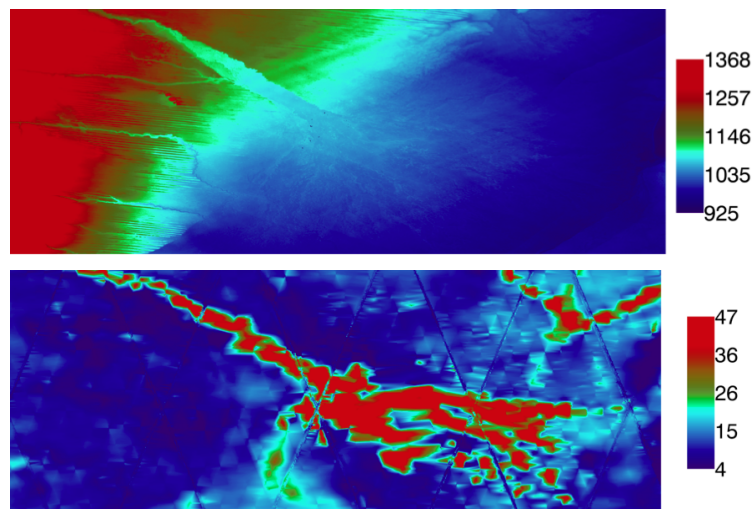


Figure 26: Height retrieval from computer simulated 20Hz data: estuarine scenario compared with input DEM

The copyright in this document is vested in SAMOSA project partners This document may only be reproduced in whole or in part, or stored in a retrieval system, or transmitted in any form (electronic, mechanical, photocopying or otherwise), only with the prior written permission of All SAMOSA project partners

Finally, a wetlands scenario was created using the Okavango delta **Figure 27**. This combined intricate DEM variation with very variable sigma0 characteristics, increasing the complexity of the model to test waveform response to variations in sigma0, whilst keeping the DEM variation within the simulator's capability. The LRM waveforms produced by the simulator were analysed, and were not found to show the expected response to the high frequency sigma0 variability in the input. Unexpectedly, no quasi-specular echoes were identified and 80% of the LRM waveforms were successfully retracked. Again, the SAR L1B 20Hz data were also analysed; the initial results were very promising, and accordingly it was attempted to retrack the SAR FBR echoes at full resolution. 40,675 waveforms were successfully retracked (62%). **Figure 28** shows a subset of the height profile for SAR FBR retracked waveforms together with the corresponding DEM input values. The FBR heights were found to closely match those of the input DEM, though the higher frequency variability was not captured. Tests to investigate the impact of the sigma0 variability on the waveforms showed little sensitivity in either amplitude or waveform width.



**Figure 27: Model inputs for wetlands scenario: DEM (top) and sigma0 (bottom)**

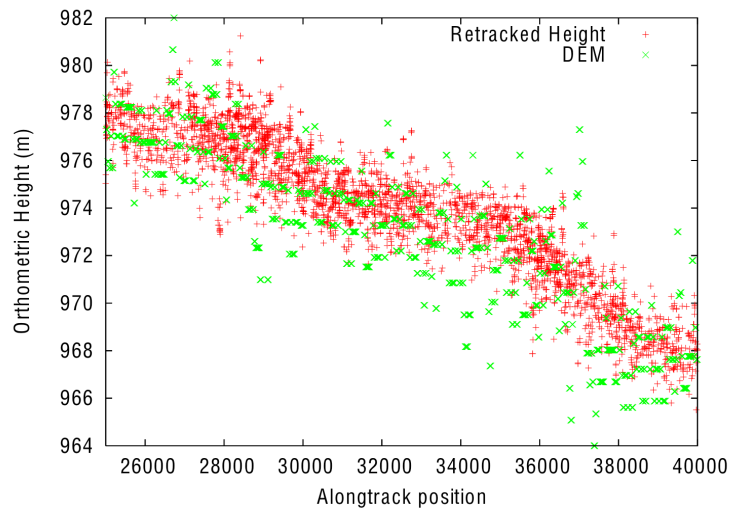


**Figure 28: SAR Full Bit Rate (no waveform averaging) retracked heights with DEM heights.**

*The copyright in this document is vested in SAMOSA project partners This document may only be reproduced in whole or in part, or stored in a retrieval system, or transmitted in any form (electronic, mechanical, photocopying or otherwise), only with the prior written permission of All SAMOSA project partners*

The results from this work were extremely positive, and indicated that much valuable information could potentially be gleaned by stacking and multi-looking the SAR FBR waveforms. However, results from the 'real Earth' are expected to be more complex and diverse than those from a simulator, and so the final part of this work involved a first look at CryoSat2 data. A typical example result from the Northern USA (-78.87304W to -81.58107 W; 49.92901N to 29.12362N) is shown for the LRM waveforms in **Error! Reference source not found.**

For this sequence, the waveforms show clear distortion and ghosting, with individual waveforms showing numerous power returns meaning that retracking is often impossible. These endemic anomalies, which it is considered may be residual processing artefacts, have restricted the scope of inland water analysis from the currently available CryoSat2 data.

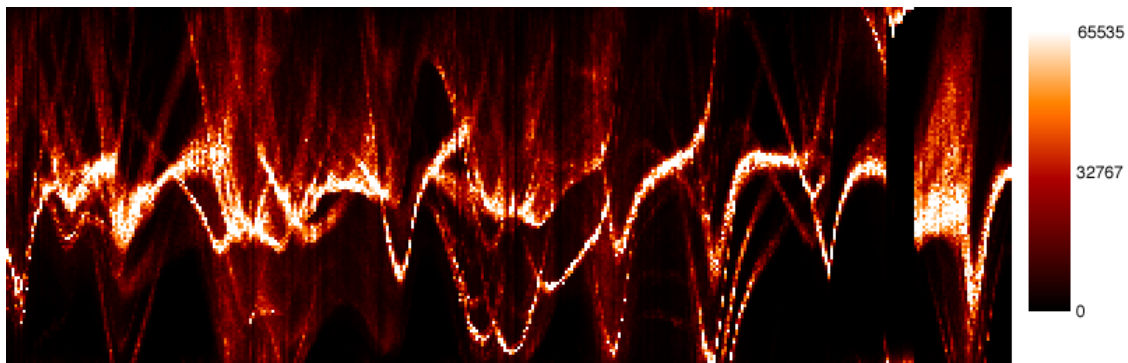


**Figure 29: Cryosat-2 LRM waveform sequence**

Availability of Cryosat-2 Level 1 FBR data over non-cryospheric land is limited, but is available over the Mekong River and its surrounding land area (**Figure 30**). FBR data from two passes were analysed to determine whether the waveform characteristics matched those of the simulator, and if they could be successfully tracked.

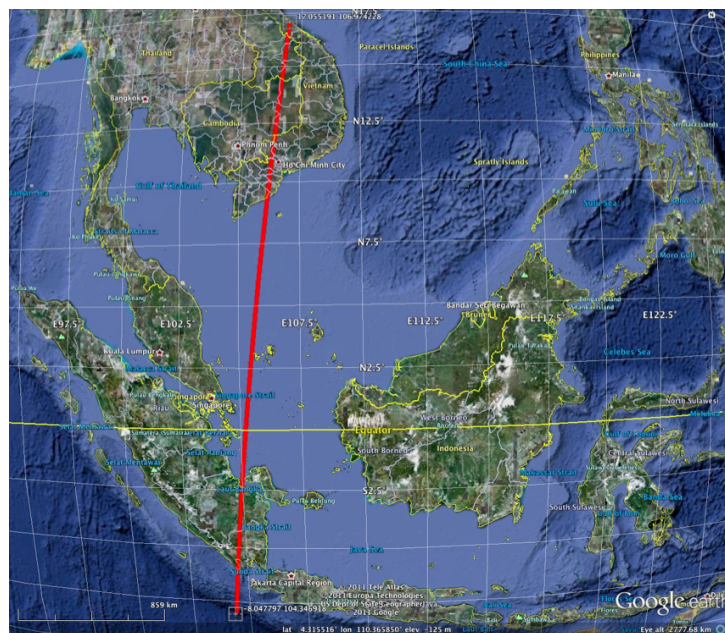


**Figure 30: Cryosat-2 track over the Mekong River region for which FBR data are available**

**Figure 31** provides an example section of waveforms from this pass. Quasi-specular waveforms are in evidence throughout the data, and other waveforms show power across a number of bins increasing the complexity of re-tracking. This behaviour is different from that found in the simulated data, but closer to that expected from a surface with a highly variable  $\sigma_0$ . Between 58-60% of the waveforms could be

*The copyright in this document is vested in SAMOSA project partners This document may only be reproduced in whole or in part, or stored in a retrieval system, or transmitted in any form (electronic, mechanical, photocopying or otherwise), only with the prior written permission of All SAMOSA project partners*

successfully re-tracked

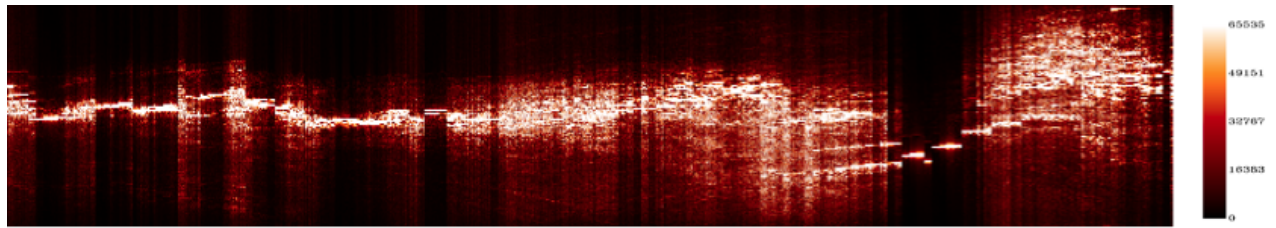


**Figure 31: Cryosat-2 SAR FBR waveforms from the track over the Mekong River region**

In summary, simulated SAR data were generated for scenarios representing inland waters, including a lake scenario, an estuarine scenario and a wetland scenario. These were processed with BEST and successful retracking of the SAR waveforms (more than 62% for the wetland, and up to 85% for the lake scenario) and recovery of small scale topographic features was demonstrated. However, there was an unexpected lack of response to variability in  $\sigma_0$

The analysis of real data from CryoSat-2 is encouraging. Many more quasi-specular targets were identified than were present in the wetlands scenario output. In this regard the ‘real’ waveform shapes conformed much more closely to those predicted on the basis of extensive work with the EnviSat Burst Echoes, than the CRYMPS output waveforms. The majority of real waveforms could be successfully retracked with no averaging, however there does appear to be significant mirroring occurring within the waveforms which will impact the ability to retrack. These features are assumed to be remaining artefacts in the CryoSat2 processing, since no trace of this phenomenon was seen in any CRYMPS waveform sequences. Thus it is concluded that this was not an expected feature of SAR FBR waveform sequences.

This work has provided a valuable insight into how an altimeter in SAR FBR mode will perform over a wetland/river network. As with previous altimeters the waveforms returned over land are far more varied and complex than those produced over the open ocean, however with the correct retracking, useable heights can be derived even with no averaging at extremely high PRF.

*The copyright in this document is vested in SAMOSA project partners This document may only be reproduced in whole or in part, or stored in a retrieval system, or transmitted in any form (electronic, mechanical, photocopying or otherwise), only with the prior written permission of All SAMOSA project partners*

## 6 Conclusions

### 6.1 Summary of Results

The SAMOSA project team succeeded in defining novel retracking techniques for SAR Mode (SARM) altimeter echoes over water surfaces and in evaluating the performance of SARM altimetry compared to conventional pulse-limited altimetry. The performance of SARM in terms of range retrieval accuracy was analysed by retracking simulated Cryosat data, airborne data and CryoSat-2 data, and with estimates of achievable precision of SARM through the Cramér-Rao Lower Bound (CRLB) method. In addition, the “Berry Expert System” (BEST) was also applied to simulated data over complex inland water scenarios to assess SARM performance over lakes, estuarine and wetlands. Key developments and results are described here.

The SAMOSA project led to the definition of two new theoretical models for SAR waveforms over water. The first model (“SAMOSA1”) assumes Gaussian ocean wave statistics and a circular antenna pattern, and includes the effect of Earth curvature and antenna mispointing in the along track direction only. An enhancement of the SAMOSA1 formulation (“SAMOSA1\_Enhanced”) addresses numerical singularities in the trailing edge of the SAMOSA1 SAR waveforms in low sea state conditions. The SAMOSA1 Enhancement allows waveform fitting to use data over the full gate range and produces an almost ten-fold reduction in computation time. The SAMOSA2 SAR model is a more complex formulation that includes non-Gaussian ocean wave statistics, Earth curvature and a better representation of mispointing effects both along- and across-track. The SAMOSA2 model also comprises radial velocity effects and an elliptical antenna pattern. All SAMOSA theoretical models were implemented as SAR ocean retracker and applied successfully to simulated and CryoSat-2 SAR waveforms.

The SAMOSA1 SAR ocean retracker was documented in a Detailed Processing Model (DPM) in support of the Sentinel-3 Surface Topography Mission (S-3 STM). The DPM was based on the original SAMOSA1 formulation and did not include the more recent enhancements of the SAMOSA1 model in low sea states.

Waveform retracking applied to simulated Cryosat data over ocean surfaces allowed for quantitative comparison of “Low Rate Mode” (LRM - conventional altimeter approach) and “SAR mode” (SARM) over identical sea state conditions. The SAMOSA1 SAR ocean retracker was applied to simulated SARM data to estimate the retrieval accuracy for range and significant wave height (SWH) in SAR mode, while LRM waveforms for the same ocean surfaces were retracked using a Brown-type ocean retracker. A technique was developed for the reduction of SARM data to emulate LRM and implemented in the “RDSAR” software. Retracking the “pseudo-LRM” RDSAR waveforms with a Brown-type ocean retracker showed that the RDSAR data offer the same retrieval accuracy than LRM. This work also showed an almost two-fold improvement in range retrieval with SARM compared to LRM and RDSAR, thus confirming earlier results from [RAN1998]. However, results with simulated data were not fully conclusive as no improvement was found in the retrieval of SWH from SARM data compared to conventional altimetry.

The SAMOSA1 ocean retracker performance was evaluated against airborne SAR altimeter data acquired with ASIRAS during the Cryovex’2006 campaign. Over 96% of the waveforms were successfully fitted by the SAMOSA1 model when the ASIRAS data was processed to have 64 pulses per burst and a maximum look angle of 1.4 degrees.

The SAMOSA1 Enhanced model was used to successfully retrack real Cryosat-2 SAR waveform data from different oceanic regions. The retrieval accuracy of SAR and LRM in different sea states was estimated for range and significant wave height using Cryosat-2 SAR and Jason-2 LRM data from a small region of the Norwegian Sea between July 2010 and March 2011. Results confirmed a marked, almost two-fold, improvement in range retrieval accuracy with Cryosat-2 SAR compared to Jason-2 LRM. Results also indicated that retrieval of significant wave height is at least as good for SARM as for LRM, although SARM overestimated SWH slightly compared to LRM, particularly in low sea states.

The SAMOSA2 waveform model was also implemented as a SAR ocean retracker and applied to simulated data and a small number of CryoSat-2 L1B SAR waveforms. The SAMOSA2 waveform model being more complex, it required longer computation time than SAMOSA1. Consequently, there was insufficient time within the project schedule to fully evaluate the performance of the SAMOSA2 retracker against Cryosat-2 data. Results with SAMOSA2 applied to simulated SAR data confirmed the findings with

*The copyright in this document is vested in SAMOSA project partners This document may only be reproduced in whole or in part, or stored in a retrieval system, or transmitted in any form (electronic, mechanical, photocopying or otherwise), only with the prior written permission of All SAMOSA project partners*

SAMOSAS1 of an approximately two-fold improvement in range retrieval accuracy with SAR compared to LRM. Analytical solutions have been identified to speed-up the computation of SAMOSA2 and could be incorporated in future implementations.

The performance of both SAMOSA1 and SAMOSA2 models were evaluated numerically in terms of precision with Cramér-Rao Lower Bound techniques. The SAMOSA2 model was found to be more robust than SAMOSA1. The impact of the various model improvements was investigated and quantified separately in terms of their effect on the precision of range retrieval. The modification of the model to include non-Gaussian ocean statistics had the greatest effect on precision. However, the change in precision resulting from these improvements was found to be small in terms of the overall precision error budget.

Simulated LRM and SARM data were obtained also for scenarios representing inland waters, including a lake scenario, an estuarine scenario and a wetland scenario. These were processed with BEST and successful retracking of the SAR waveforms (more than 62% for the wetland, and up to 85% for the lake scenario) and recovery of small scale topographic features was demonstrated. However, the simulated data did not show the expected response to variability in the input  $\sigma_0$ . Analysis of real Cryosat-2 SAR data over the Mekong River region was encouraging. Quasi-Specular echoes were identified, as expected, and approximately 60% of waveforms were successfully retracked, though there appeared to be significant mirroring within the waveforms, which affects the ability to re-track these data.

In summary, the SAMOSA project successfully demonstrated the potential improvements offered by SAR mode altimetry over water surfaces. Through the development of new theoretical models for SAR waveforms over water and their application as SAR ocean altimeter retrackerers to simulated and real Cryosat-2 L1B SAR data, SAMOSA confirmed earlier expectations of improvement in range retrieval accuracy and finer along-track spatial resolution.

## 6.2 Recommendations for Further Work

Further work is recommended to build on the progress made within the SAMOSA contract to resolve some known issues, establish a more complete understanding of the performance of SAR mode altimetry over water and to work towards operational implementations of SAR retrackerers for these data. In particular the following activities are advised:

- More efficient software implementation of the SAMOSA2 retracker
- Validation and testing of the SAMOSA SAR retrackerers with a wider range of Cryosat-2 data co-located with ground truth and/or other reference data. This should include analysis of range, significant wave height and  $\sigma_0$  performance.
- Update the DPM to include (at least) the SAMOSA1 Enhancement to resolve the numerical singularities at low wave heights and allow retracking over the full range of waveform gates.
- Cross validation of the SAMOSA results with simulated Cryosat data against output from the Sentinel-3 mission simulator for the same scenarios.
- Benchmark testing of SAMOSA retrackerers with other approaches. For example, the SAMOSA team is aware of an alternative method proposed by [JEN1999] involving non-uniform weighted gates. This method performs a transformation of the delay Doppler altimeter echoes into Brown-type ocean waveforms, thus offering the significant practical advantages of allowing retracking with systems inherited from conventional altimetry. To date, the SAMOSA team has not had the opportunity to compare Jensen's approach with the SAMOSA theoretical retracking method and thus cannot conclude on which method offers the better performance. It is noted that Jensen's approach involves a waveform shape transformation, which may degrade some of the geophysical information contained in the waveform shape. Thus, benchmark testing of the two approaches with the same datasets is required to gather evidence upon which to base any firm conclusions.
- Validation of the RDSAR technique to reduce SAR mode to Low Rate mode data using real data, to prepare for its application to Sentinel-3 data and provide continuity over the altimeter SAR/LRM mode transitions. This analysis should include the re-tracking of Cryosat-2 data over an area of ocean where statistics are consistent over an area of 100s km and where the altimeter switches

*The copyright in this document is vested in SAMOSA project partners This document may only be reproduced in whole or in part, or stored in a retrieval system, or transmitted in any form (electronic, mechanical, photocopying or otherwise), only with the prior written permission of All SAMOSA project partners*

between LRM and SAR. Performance should be assessed on a large scale statistical basis as well as thorough consideration of individual along track profiles.

### **6.3 Acknowledgements**

The SAMOSA team would like to express its appreciation to all those who have contributed to the success of the project through useful and constructive discussions. In particular we are grateful to Prof Keith Raney of Johns Hopkins University for his important input throughout the project and for travelling to attend many of the project meetings.

We would also like to thank the ESA project management team who have provided strong technical insight and always been very supportive and shown flexibility to allow the team to adapt its plans according to new developments.

*The copyright in this document is vested in SAMOSA project partners This document may only be reproduced in whole or in part, or stored in a retrieval system, or transmitted in any form (electronic, mechanical, photocopying or otherwise), only with the prior written permission of All SAMOSA project partners*

## Bibliography

- RAN1998: Raney, R. K., The Delay/Doppler Radar Altimeter, IEEE Trans. Geosci. Remote Sensing, vol. 36, pp. 1578-1588, Sept.1998.
- RAN1994: Raney, R. K., Precision SAR Processing Using Chirp Scaling, IEEE Trans. Geosci. Remote Sensing, vol. 32, pp. 786-799, Jul. 1994.
- BRO1977: Brown, G.S, The average impulse response of rough surface and its applications, 1977
- HAY1980: Hayne, G.S, Radar altimeter mean return waveform from near-normal-incidence ocean surface scattering , 1980
- JEN1999: Jensen, J.R., Radar Altimeter Gate Tracking: Theory and Extension, 1999
- CMP2008: Martin-Puig, C. and G. Ruffini, Theoretical Model for SAR altimeter mode processed echoes over ocean surfaces - revised, SAMOSA, WP4 - TN - STARLAB, 2008
- CMP2009: Martin-Puig, C. and G. Ruffini, SAR Altimeter Mean Return Waveform from Near-normal-incidence ocean surface scattering, SAMOSA, WP5 - TN - STARLAB, 2009
- RAY2011: Ray, C., C. Martin-Puig, G. Ruffini, Further development of SAR altimeter waveform model, SAMOSA CCN, WP3100 - D8 - STARLAB, 2011
- CMP2010: Martin-Puig, C. and J. Marquez, RDSAR Software Documentation, 2010
- MAV2004: Mavrocordatos, C., E. Attema, M. Davidson, H. Lentz and U. Nixdorf, Development of ASIRAS (Airborne SAR/Interferometric altimeter system), 2004
- STE2007: Stenseng, L., S.M. Hvidegaard, H. Skourup, R. Forsberg, C.J. Andersen, S. Hanson, R. Cullen and V. Helm, Airborne lidar and radar measurements in and around Greenland, CryoVEx 2006, TR9 - DTU, 2007
- CUL2010: Cullen, R., CryoVex Airborne Data Product Description. , 2010
- AND2009: Andersen, O.B and P. Knudsen, DNSC08 mean sea surface and mean dynamic topography models, 2009
- ABD2011: Abdalla, S., ECMWF wave model Position of (78.1N, 3.4W) on 30th April 2006, 2011
- STE2009: Stenseng, L., Validation using airborne ASIRAS data , SAMOSA, WP8 - D8 - DTU, 2009
- STE2011: Stenseng, L. and C. Gommenginger, Validation against ASIRAS, SAMOSA CCN, WP2300 - D6 - DTU/NOC, 2011
- GOM2011: Gommenginger, C., Martin-Puig , C., Srokosz, M., Caparrini, M., Dinardo, S., Lucas, B. & J. Benveniste: Detailed Processing Model of the Sentinel-3 SRAL SAR altimeter ocean waveform retracker, Version 1.3.1, 21 June 2010. ESRIN Contract No. 20698/07/I-LG "Development of SAR Altimetry Mode Studies and Applications over Ocean, Coastal Zones and Inland Water" (SAMOSA), 63 pages, 2010.

*The copyright in this document is vested in SAMOSA project partners This document may only be reproduced in whole or in part, or stored in a retrieval system, or transmitted in any form (electronic, mechanical, photocopying or otherwise), only with the prior written permission of All SAMOSA project partners*

## List of SAMOSA Publications

Below we list in chronological order all the scientific papers and conference presentations made by members of the SAMOSA team, in which they have presented results from the SAMOSA project.

1. Martin-Puig, C., Marquez, J., Ruffini, G., Raney, K.R., and Benveniste, J., 2008, SAR Altimetry Applications Over Water, ESA SeaSAR Workshop, 21-25 January 2008.
2. Gommenginger, C., Cipollini, P., Martin-Puig, C., Marquez, J., Cotton, P.D., Raney, K.R., and Benveniste, J., 2008, SAR Altimetry Numerical Simulations over Water Surfaces, presented at EGU General Assembly 2008, Vienna, Austria, 13-18 April 2008. Abstract in Geophysical Research Abstracts, Vol. 10, EGU2008-A-08929, 2008..
3. Martin-Puig, C., Marquez, J., Ruffini, G., Cotton, P.D., Gommenginger, G., Challenor, P.G., Raney, K.R., and Benveniste, J., 2008, New Theoretical Model of SAR Altimeter Signal Over Water Surfaces, IGARSS, 7-11 July 2008.
4. Cotton, P.D., Benveniste, J., Andersen O., Stenseng, L., Berry, P., Cipollini, P., Gommenginger, G., Martin-Puig, C., and Raney, K.R., 2009, Investigating the Application of Synthetic Aperture Altimetry over oceans, coastal and inland waters. presented at EGU 2009 General Assembly, Vienna, Austria, 20-24 April 2009. Abstract in Geophysical Research Abstracts, Vol. 11, EGU2009-10680, 2009.
5. Gommenginger, C., Martin-Puig, C., Cotton, P.D., Raney, K.R., and Benveniste, J., 2009, Assessing the Altimetric Precision of Delay Doppler Altimetry Over the Ocean With Numerical Simulations From the Cryosat Mission Performance Simulator, IGARSS July 12-17 2009.
6. Gommenginger, C., Martin-Puig, C., Cotton, P.D., Dinardo, S., and Benveniste, J., 2010, A prototype SAR altimeter retracker to assess the precision of SAR altimetry over the ocean. ESA SeaSAR Workshop 25-29 January 2010.
7. Martin-Puig, C., Andersen O., Berry, P., Cipollini, P., Cotton, P.D., Gommenginger, Ruffini, G., G., Stenseng, L., Benveniste, J., and Dinardo, S., 2010, SAR Altimetry Over Water Surfaces, poster presented at Oceans from Space – Venice 2010, Venice, Italy, 26-30 April 2010. (Abstract in proceedings, pp. 161-162).
8. Gommenginger, C., Martin-Puig, C., Dinardo, S., Raney, K. R., Cotton, P.D., and Benveniste, J., On the altimetric performance of the Sentinel-3 SAR-mode altimeter over the ocean: a numerical study. EGU 2-7 May 2010.
9. Martin-Puig, C., Marquez, J., and Gommenginger, C., 2010, CryoSat-2: From SAR FBR to LRM for quantitative precision comparison over identical sea state. ESA Living Planet Symposium 28 June – 2 July 2010.
10. Cotton, P.D., Andersen O., Berry, P., Cipollini, P., Gommenginger, G., Martin-Puig, C., Stenseng, L., Benveniste, J., and Dinardo, S., 2010, The SAMOSA Project: Assessing the Potential Improvements offered by SAR Altimetry Over the Open Ocean, Coastal Waters, Rivers and Lakes. ESA Living Planet Symposium 28 June – 2 July 2010.
11. Martin-Puig, C., Marquez, J., Ruffini, G., Raney, K.R., and Gommenginger, C., 2010, CryoSat-2: From SAR to LRM (FBR) for quantitative precision comparison over identical sea state, COSPAR 18-25 July 2010.
12. Gommenginger, C., 2010, Improved spatial resolution and range retrieval accuracy with SAR altimeters over the ocean and the coastal zone: a numerical study, Altimetry for Oceans and Hydrology OST-ST Meeting 18-22 October 2010.
13. Gommenginger, C. 2010, On the Performance of CryoSat-2 SAR Mode over Water Surfaces, Cryosat 2011 Workshop, ESRIN, Frascati, 1-3 February 2011
14. Stenseng, L. 2010, First Results of Recovery of Short Wavelength Gravity Field Signals from CryoSat-2 Data. Cryosat 2011 Workshop, ESRIN, Frascati, 1-3 February 2011
15. Gommenginger, G., Martin-Puig, C., Dinardo, S., Raney, K.R. Cotton, P.D., and Benveniste, J., 2011, An Open Ocean Retracker for Sentinel-3 and Cryosat Altimeter Waveforms, presented at EGU 2011 General Assembly, Vienna, Austria, 03-08 April 2011. Abstract in Geophysical Research Abstracts, Vol. 13, EGU2011-3742-1, 2011.

*The copyright in this document is vested in SAMOSA project partners This document may only be reproduced in whole or in part, or stored in a retrieval system, or transmitted in any form (electronic, mechanical, photocopying or otherwise), only with the prior written permission of All SAMOSA project partners*

# Annex 1: Commentary on the SAMOSA Project, Final Presentation by Dr R. K. Raney, Johns Hopkins University, Applied Physics Laboratory

2<sup>nd</sup> June 2011

1. In general, it was good to hear about the progress that the SAMOSA Team has made on interesting and sometimes challenging problems raised by pressing the potential capabilities, limitations, and processing issues presented by the data from SAR-mode radar altimeter architectures.

2. It is noted that the history of oceanic radar altimetry offers opportunities to place in appropriate perspective what has been accomplished, what we may try to achieve in future, and the time scales for these steps. For reference, an Annotated Bibliography is attached to this commentary. The history of the traditional approach to observing the ocean's surface by a nadir-viewing radar shows that it required more than 20 years for a rudimentary understanding of the ocean's response function (1957) to evolve into an operational methodology (early 1980s) for extracting the parameters of interest (principally SSH, SWH, and WS) from the radar's returns.

3. As the Sentinel-3 era approaches, there are those who are eager (as was evident at the SAMOSA Final Review) to have in place operational algorithms for parameter retrieval from SAR-mode altimeter data. Patience is advised. The concept of a combined "pulse-limited and beam-limited" radar has been known to the wider community for only about 13 years, and real data from such an orbital radar (CryoSat-2) has been available for less than one year. Considerable progress has been made by the SAMOSA team and others, but at present there is no consensus on methods, potentials, or limitations associated with parameter retrievals from such a radar.

4. SAR-mode data from an inclined orbit over the global oceans could lead to a two-octave improvement of the spatial scale of retrieved bathymetry. CryoSat-2 data could be exploited to verify this expectation, at least on a small scale. Further, it may be possible for the CryoSat-2 simulator to generate sufficient data to put this claim to the test, although there may still linger concerns about the suitability of such data for this application, which falls outside of the intended purpose for that facility.

5. Tracking and re-tracking approaches seem to be converging, based on exercises with simulated as well as actual SAR-mode data.

6. Efforts within SAMOSA to transform SAR-mode data (either from simulated data sequences or from actual CryoSat data) into pseudo-LRM data have been successful, passing quantitative statistical tests for their acceptance. This tool should be valuable for comparative evaluations of retrievals from the two modes over a variety of oceanic conditions.

7. Results seem to show consistently that the precision of SSH retrieval from SAR-mode data is significantly better (by approximately a factor of 2) than for retrievals from LRM data. This is in line with early predictions and simulation studies.

8. Retrievals from SARM and pseudo-LRM claimed to have less consistency for SWH retrievals. This may be due to the lack of "fit" between the model and the data for the tails (later time delays) of the waveform distributions. The "width" of the model profile when fitted to the data depends on the fit at the later time delays. Convergence between the model and the data on this aspect should lead to improvements. One way to approach that goal could be to adapt the Jensen re-tracking method to the problem, since the first step in that method is to transform the SARM peaky (hybrid pulse- and beam-limited) waveform into a Brown-style pseudo-pulse-limited waveform.

9. It was argued that the reason for the very high PRF (~18 kHz) in SARM is to assure correlation between adjacent pulses. Strictly speaking, this argument is not correct. Once the PRF is well above the WALSH limit (~2500 kHz), correlation from a user's point of view is guaranteed. The reason for the high PRF in SARM is to assure that the Doppler spectrum across the antenna pattern is adequately sampled. If the PRF is above the Doppler band width, then the Nyquist lower bound on sampling rate is satisfied. This is purely a radar argument. The Nyquist lower bound assures that there will be minimal ambiguities in the

*The copyright in this document is vested in SAMOSA project partners. This document may only be reproduced in whole or in part, or stored in a retrieval system, or transmitted in any form (electronic, mechanical, photocopying or otherwise), only with the prior written permission of All SAMOSA project partners.*

sampled data; it has nothing to do with the inherent correlation within the signal stream due to the properties of the observed scene.

10. The sampling rate question is central to the design and performance of a SAR mode altimeter. The question was addressed in a paper presented at the ESA Living Planet symposium (Bergen, Norway, 2010), a copy of which is attached to this commentary. The main theme of that paper is that future designs of a SAR-mode ocean-viewing altimeter could realize about three times as many statistically independent looks than are possible from the design approach taken for CryoSat.

11. The summary of detailed studies on the tracking and sampling properties of the ASIRIS airborne instrument was informative. The bottom line is that IF an airborne system is to generate data that are similar to those gathered by the intended orbital instrument, THEN the dominant requirement on the airborne system is to replicate as closely as possible (given the limitations of the aircraft's speed and altitude) the geometrical parameters at the surface for the two data sets. These include in particular incidence and footprint resolution. Analysis of ASIRIS data revealed that its very fine along-track resolution (a few meters in contrast to CryoSat's ~200 m) and large off-nadir incidence (~45° in contrast to CryoSat's ~2°) both induced unacceptable behavior in the resulting data.

*The copyright in this document is vested in SAMOSA project partners This document may only be reproduced in whole or in part, or stored in a retrieval system, or transmitted in any form (electronic, mechanical, photocopying or otherwise), only with the prior written permission of All SAMOSA project partners*

# Annex 2: An Annotated Bibliography: Selected Milestones of oceanic radar altimetry leading to finer height precision and the Cryosat Heritage by Dr R. K. Raney, Johns Hopkins University, Applied Physics Laboratory

2<sup>nd</sup> June 2011

[1] R. K. Moore and C. S. Williams, Jr., "Radar return at near-vertical incidence," Proceedings of the IRE, vol. 45, pp. 228-238, 1957.

*The first treatment of the impulse response of a radar looking at a quasi-smooth horizontal surface from above, introducing the "beam-limited" and the "pulse-limited" waveforms and their associated radar power equation. The pulse-limited form since then has been the norm for orbital ocean-viewing altimeters. Beam-limited waveforms are "peaky", in contrast to the pulse-limited response, which is, to first order, a step function.*

[2] W. J. J. Caputi, "Stretch: a time-transformation technique," IEEE Transactions on Aerospace and Electronic Systems, vol. AES-7, pp. 269-278, 1971.

*Stretch is a clever technique whereby a short objective range window observed by a radar at very long range may be traded (conserving the pulse's time-bandwidth product) such that a linear fm signal from the intended window may be stretched over much of the unused range time, thus vastly reducing its fm rate and bandwidth, which enables subsequent real rate data processing.*

[3] J. L. MacArthur, "Design of the Seasat-A radar altimeter," Oceans, vol. 8, pp. 222-229, 1976.

*MacArthur introduced the Stretch technique into radar altimetry, changing its name to "full de-ramp" (without appropriately acknowledging Caputi). The method was first used on the Seasat altimeter (1978), and since then has been the method of choice for oceanographic altimetry. It is the main reason that bandwidths on the order of 300 MHz (and their associated 0.5-m single pulse range resolution) submit to extensive on-board processing.*

[4] G. S. Brown, "The average impulse response of a rough surface and its applications," IEEE Antennas and Propagation, vol. 25, pp. 67-74, 1977.

*Brown generalized Moore's pulse-limited impulse response, casting it as the convolution of three fundamental transfer functions, one of which represented the characteristics of the reflecting surface. This paper is the genesis of the "Brown model", from which tracking (and re-tracking) algorithms extract the three principal parameters SSH, SWH, and WS. (By the way, precision oceanic altimetry was at the time a sensitive issue, because improved knowledge of the global geoid had strategic implications. Gary once told me that one of his papers was re-classified above his clearance level, so that he had to forfeit all copies of it, and he was barred from reading his own work.)*

[5] G. S. Hayne, "Radar altimeter mean return waveforms from near-normal incidence ocean surface scattering," IEEE Antennas and Propagation, vol. AP-28, pp. 687-692, 1980.

*This paper was one of a expanding series that contributed to transforming radar altimetry from a challenging academic exercise into an operational tool. Parameter extraction using Brown's model was the backbone of the technique.*

[6] W. F. Townsend, "An initial assessment of the performance achieved by the Seasat-1 radar altimeter," IEEE Journal of Oceanic Engineering, vol. OE-5, pp. 80-92, 1980.

*This paper provides a concise review of the successful demonstration of the Seasat radar altimeter .*

[7] E. J. Walsh, "Pulse-to-pulse correlation [7] E. J. Walsh, "Pulse-to-pulse correlation in satellite radar altimetry," Radio Science, vol. 17, pp. 786-800, 1982.

*Early experiments (using the rudimentary proof-of-concept altimeter on SkyLab) varied the radar's pulse*

*The copyright in this document is vested in SAMOSA project partners This document may only be reproduced in whole or in part, or stored in a retrieval system, or transmitted in any form (electronic, mechanical, photocopying or otherwise), only with the prior written permission of All SAMOSA project partners*

repetition frequency (prf). Walsh' paper summarizes the results, which showed that correlation is introduced between successive returns if the prf is too high. As the primary benefit of averaging was to reduce the standard deviation of parameters derived from the waveform ensemble, such correlation was not wanted. This paper presents an analytical form for the threshold condition, known as the Walsh upper bound on prf.

[8] J. L. MacArthur, P. C. Marth, and J. G. Wall, "The GEOSAT Radar Altimeter," Johns Hopkins APL Technical Digest, vol. 8, pp. 176-181, 1987.

*This paper describes the design of the Geosat radar altimeter, the first dedicated oceanographic mission. The first 18 months of the mission were in a non-repeating orbit, intended to collect data sufficient to establish the ocean's geoid (on scales larger than about 20 km), and as such those data were classified for nearly ten years.*

[9] D. B. Chelton, E. J. Walsh, and J. L. MacArthur, "Pulse compression and sea-level tracking in satellite altimetry," Journal of Atmospheric and Oceanic Technology, vol. 6, pp. 407-438, 1989.

*This is a classic altimetry paper, co-authored by a multi-disciplinary team of leading individuals (at the time): a radar altimeter engineer (MacArthur), a waveform practitioner (Walsh), and a user of the data (Chelton).*

[10] A. R. Zieger, D. W. Hancock, G. S. Hayne, and C. L. Purdy, "NASA radar altimeter for the TOPEX/Poseidon project," Proceedings of the IEEE, vol. 79, pp. 810-826, 1991.

*Thanks to promotion to a new level (literally) by influentials such as Carl Wunsch, radar altimetry was the basis of a new series of dedicated mission aimed at long-term observation of the status and changes in the sea surface topography. This paper describes in some detail the design of the TOPEX altimeter, which was based extensively on the Seasat and Geosat precedents, but included several significant advances.*

[11] P. C. Marth, J. R. Jensen, C. C. Kilgus, J. A. Perschy, J. L. MacArthur, D. W. Hancock, G. S. Hayne, C. L. Purdy, L. C. Rossi, and C. J. Koblinsky, "Prelaunch performance of the NASA altimeter for the TOPEX/Poseidon Project," IEEE Transactions on Geoscience and Remote Sensing, vol. 31, pp. 315-332, 1993.

*In similar spirit as that preceding, this paper looked at the performance expected from the TOPEX mission.*

[12] W. H. F. Smith and D. T. Sandwell, "Bathymetric prediction from dense satellite altimetry and sparse shipboard bathymetry," J. Geophys. Res., vol. 99, pp. 21803-21824, 1994.

*Once the geodetic data from Geosat were declassified, then academics such as Smith and Sandwell could publish their methodology and results on measuring the sea surface topography, and, of most interest to many, their back-propagation techniques for estimating the sea's bottom topography and its corresponding depth contours. Geosat data (aided by ERS-1 altimeter data from its long repeat cycle mode) lead to bathymetric charts down to about 20-km spatial scales.*

[13] J. R. Jensen, "Design and performance analysis of a phase-monopulse radar altimeter for continental ice sheet monitoring," in Proceedings, IEEE International Geoscience and Remote Sensing Symposium IGARSS'95. Florence, Italy: IEEE, 1995, pp. 865-867.

*Over the previous two decades there had been several studies seeking ways to extend the useful swath of a radar altimeter beyond the limits of the nadir (sub-satellite) track. This was the first paper to use the interferometric (phase-monopulse) technique to measure and then to correct for the height error induced by a cross-track slope of the intended surface.*

[14] R. K. Raney, "The delay Doppler radar altimeter," IEEE Transactions on Geoscience and Remote Sensing, vol. 36, pp. 1578-1588, 1998.

*Expanding on a previous conference paper (IGARSS'95), this was the first journal publication of a synthetic aperture radar approach to oceanic altimetry. In perspective, the result of the delay-Doppler processing described in the paper was a new altimeter architecture in which the cross-track impulse response was pulse-limited, whereas the along-track response was beam-limited. In this case, the beam was limited by its Doppler bandwidth (and offset), which were determined by specific properties of the radar design.*

[15] D. J. Wingham, et al., "CryoSat: A Mission to Determine Fluctuations in the Mass of the Earth's Land

*The copyright in this document is vested in SAMOSA project partners. This document may only be reproduced in whole or in part, or stored in a retrieval system, or transmitted in any form (electronic, mechanical, photocopying or otherwise), only with the prior written permission of All SAMOSA project partners.*

and Marine Ice Fields," University College, London, UK, Proposal to the European Space Agency October 1998.

*The CryoSat radar was based on a design that combined the methods of the previous two papers. Although such an instrument had been unsuccessfully proposed to NASA (1996), the Wingham proposal, which was based on a solid science rationale, became the first ESA Earth Explorer mission.*

[16] J. R. Jensen and R. K. Raney, "Delay Doppler radar altimeter: Better measurement precision," in Proceedings IEEE Geoscience and Remote Sensing Symposium IGARSS'98. Seattle, WA: IEEE, 1998, pp. 2011-2013.

*Delay-Doppler generates more statistically-independent waveforms, hence these when summed reduce the standard deviation of the retrieved parameters. This paper summarizes the results of simulations which verify the theoretical predictions.*

[17] J. R. Jensen, "Radar altimeter gate tracking: theory and extension," IEEE Transactions Geoscience and Remote Sensing, vol. 37, pp. 651-658, 1999.

*The SAR-mode (delay-Doppler) altimeter produces a class of waveform previously not seen. This paper is the first to look carefully at the tracking problems associated with this new non-Brown waveform.*

[18] C. Zelli, "ENVISAT RA-2 Advanced radar altimeter: Instrument design and pre-launch performance assessment review," Acta Astronautica, vol. 44, pp. 323-333, 1999.

*In contrast to operational oceanic radar altimeters which perform tracking and first-order waveform summing on board, the RA-2 was the first to introduce an experimental mode in which short bursts of data in full detail were collected and relayed to the ground prior to processing.*

[19] L.-L. Fu and A. Cazanave, Satellite Altimetry and the Earth Sciences, Academic Press, 2001, pp. 463.

*The state of the art (prior to CryoSat) is elegantly summarized in the Fu and Cazanave book.*

[20] W. H. F. Smith, D. T. Sandwell, and R. K. Raney, "Bathymetry from space: technologies and applications," in Proceedings MTS/IEEE Oceans 2005. Washington, DC, 2005.

*This paper quantifies the benefits of improved SSH precision as applied to charting sea bottom topography. A plea is made for a dedicated new mission using a SAR-mode radar altimeter placed in an inclined non-repeating orbit whose data products would include both oceanographic and bathymetric applications. The resulting bathymetry would have spatial resolution down to the theoretical limit on the order of 5 kilometers.*

[ END OF DOCUMENT ]

*The copyright in this document is vested in SAMOSA project partners This document may only be reproduced in whole or in part, or stored in a retrieval system, or transmitted in any form (electronic, mechanical, photocopying or otherwise), only with the prior written permission of All SAMOSA project partners*